

### RESEARCH ARTICLE

### OPEN ACCESS

## EXPERIMENTAL INVESTIGATION OF ORIENTATION-DEPENDENT TENSILE BEHAVIOUR IN FDM-PRINTED ABS AND CF-ABS COMPONENTS

Kaustubh Pravin Joshi\*<sup>1</sup>, M. K. Chopra<sup>2</sup>

<sup>1</sup>Department of Mechanical Engineering, Sarvepalli Radhakrishnan University Bhopal, Madhya Pradesh, India.

<sup>2</sup>Department of Mechanical Engineering, RKDF Institute of Science & Technology, Sarvepalli Radhakrishnan University Bhopal, Madhya Pradesh, India.

<sup>1</sup><https://orcid.org/0000-0001-6077-2481><sup>2</sup><https://orcid.org/0009-0003-0874-133X>

Email: [\\*joshikaustubhp070@gmail.com](mailto:*joshikaustubhp070@gmail.com), [chopramk62@yahoo.co.in](mailto:chopramk62@yahoo.co.in)

### ARTICLE INFO

#### Article History

Received: December 2, 2025

Reviewed: January 05, 2026

Accepted: March 10, 2026

Published: April 30, 2026

#### Keywords:

Additive manufacturing,  
Build orientation,  
CF-ABS,  
Fused deposition modeling,  
Tensile behaviour.

### ABSTRACT

Fused Deposition Modeling is the standard commonly adopted for polymer due to its wide applications however, the mechanical properties achieved by FDM-fabricated components remain insufficient for many mechanical applications. The objective of this study was to examine the outcome of build orientation on the tensile behaviour of FDM-printed ABS and CF-ABS specimens. ABS and CF-ABS were printed in the X, Y, and Z directions. X-oriented CF-ABS printed samples exhibited the highest ultimate tensile strength (28.90 MPa) with a Young's modulus of 2296.65 MPa; whereas, significantly weaker Z-oriented showed much lower strength than other samples because of weak interlayer bonding generally presented in all Z-oriented sample. Although CF-ABS becomes stiffer and stronger in the X and Y directions, the ductility stood exactly opposite since elongation dropped from 1.06% of ABS to 0.67% of CF-ABS. Taguchi-based DOE revealed that material type and build orientation were the most significant parameters influencing tensile performance. Overall, CF-ABS improved tensile property in certain directions for an optimal condition and provides orientation-based design guidance for to optimize FDM process parameters. The novelty of this study lies in the direct experimental comparison of orientation-dependent tensile behavior between ABS and CF-ABS using a Taguchi-based DOE framework under identical processing conditions.



Copyright ©2026 by authors and Galileo Institute of Technology and Education of the Amazon (ITEGAM). This work is licensed under the Creative Commons Attribution International License (CC BY 4.0).

### I. INTRODUCTION

Additive Manufacturing (AM) has changed current manufacturing capabilities by enabling the manufacture of complex structures, reduction in material wastage and delivering immense possibilities for rapid prototyping. Unlike conventional subtractive processes, where material is removed from a workpiece of a material, additive manufacturing builds components layer-by-layer based on digital CAD models and leads to great design freedom and high material utilization. Over the past three decades, AM technologies have evolved from rapid prototyping tools to functional manufacturing processes to effective processes for producing functional end-use parts across industries including aerospace, automotive, and bio-medical and consumer electronics [1]. Among the numerous processes of additive manufacturing, Fused Deposition Modeling (FDM)/ Fused Filament Fabrication (FFF) is one of the most prevalent methods.

This is mainly due to its low-cost, high availability, and ability to process multiple types of thermoplastics. FDM operates by extruding a heated filament over a nozzle and placing it along one layer at a time over the predetermined pathway to create an object. On account of its ease of use and cost effectiveness, FDM has become a preferred choice for industrial applications requiring low-volume manufacturing and customized parts [2]. Despite the aforementioned advantages, FDM-printed parts exhibit certain mechanical limitations, particularly strong anisotropy in their material properties associated with layer-by-layer deposition. These limitations manifest as poor interlayer bonding, significant porosity and anisotropic mechanical response, which limit extensive application of FDM in

structural applications [3]. To overcome these challenges, process parameters such as layer thickness, raster angle, build orientation and reinforcement methods play major roles [4], all influencing final mechanical properties of printed parts significantly.

From basic polymer printing, FDM has evolved to include fiber-reinforced composites that bring about major improvement in the mechanical attributes. Reinforcements such as carbon fiber (CF), glass fiber (GF), and kevlar combined with thermoplastic matrices like acrylonitrile butadiene styrene (ABS) and polylactic acid (PLA) have been demonstrated to possess significantly improved stiffness, strength, and thermal resistant properties [5], [6]. Of these materials, Carbon Fiber-Reinforced ABS (CF-ABS) has been of particular interest due to its balanced mechanical attributes, ease of manufacturing and reduced warping when compared to pure ABS. CF-ABS consists of short carbon fibers in an ABS material; the result is a stiff and rigid material with increased tensile and flexural strength, but at the similar time lightweight. The addition of carbon fibers helps with load sharing efficiency and reduces heat expansion, making CF-ABS as a suitable candidate for high performance items which include aerospace components, automotive parts, and industrial tooling [7], [8].

Though, the mechanical concert of CF-ABS parts strongly depends on processing settings (mainly building orientation and fiber alignment), which affect interfacial adhesion and stress distribution in printed material [9]. Despite of CF-ABS having superior mechanical properties with respect to unfilled ABS, some challenges should be addressed for unlocking its potential in FDM applications. The main experiment lies in the anisotropic things of FDM-printed composites, wherein the properties of the fusions vary with the direction of printed deposits. Consider rephrasing to avoid repetition of FDM, parts have poorer adhesion in the Z-direction than in-plane properties (X- and Y-directions). This leads to less tensile strength and flexural strength, which makes Z prints vulnerable to delamination or breaking under pressure [10], [11].

Other considerations include the orientation and dispersion of fibers in the polymer matrix. The fiber orientation control in traditional composite fabrication processes such as injection molding or filament winding is not aligned, FDM-printed composites often suffer from random or non-uniform fiber orientations. This affects the stress allocation in-between polymer matrix and fibers of reinforcement, causing differences in mechanical property at different angles [12], [13]. Additionally, presence of voids and porosities related to insufficient melting between layers reduces the mechanical properties; thus, it is necessary to tune process parameters for enhanced interlayer bonding and reduced defects [14], [15]. Among influencing factors, build orientation is one of the supreme perilous limits affecting mechanical attributes to of FDM 3D in print parts. It governs the layer stack and how the layers bond, therefore determining strength, stiffness, and failure mechanisms.

Standard build orientations in FDM include the following: X-Orientation (Flat Build) in which the printing layers are parallel to the principal loading plane and as a result, improved layer-to-layer adhesion would be achieved at expense of out-of-plane strength. This orientation is suitable for tensile applications where higher elongation and formability are required [16-18]. Y-Orientation (Edge Build): Balances layer bond and in-plane strength, often providing the top tensile and flex assets. This is due to improved fiber orientation and stress transfer in the composite matrix [19-21]. Z-Axis (Vertical Build): This orientation is mechanically the weakest due to poor interlayer bond, hence low tensile strength and poor interlayer adhesion or build delamination tendencies. Such an orientation is, however, typically not applied for load-bearing applications [22-24]. Previous studies reported in the literature indicate that that the CF-ABS possesses higher tensile strength and flexural modulus along the Y-axis due to its improved fiber-matrix bonding and interlayer adhesion.

Furthermore, Z-oriented samples exhibit very different mechanical properties due to the significant decrease in interlayer adhesion between consecutive printed layers [25-28]. This discrepancy in performance highlights the necessity of tailoring build orientation for specific load bearing applications. The mechanical properties of FDM 3D printed ABS parts performed better because of including carbon fiber reinforcements. Improved stiffness, tensile strength and thermal stability could be attributed to carbon fibers, making CF-ABS composites promising for demanding applications. However, the level of these improvements is heavily determined by a number of considerations: Fiber Length and Content: Most FDM filaments use short carbon fibers (SCFs) sized in the range 100–500  $\mu\text{m}$ . Fiber content, from 5 to about 30% wt., has a direct influence on mechanical properties. Higher fiber content increases the stiffness and strength respectively, but may reduce the ductility due to an increase of brittleness [29-34].

Fiber Orientation: Fibers can orient themselves in line with the direction you're printing owing to extrusion. This orientation will enhance mechanical properties along the axis of the filament and may compromise strength in transversal directions. Obtaining a homogeneous strength distribution is strongly predicated on accurate fiber angles resulting from optimization of slicing [35]. Interface Bonding: The fiber/ABS matrix adhesion must also be strong to ensure efficient load transfer. Low adhesion causes fiber pulling off and premature rupture in tensile loading. Surface modifications and/ or different polymer matrices have been studied in order to increase fiber-matrix interaction and enhance mechanical performance [36-38]. In order to maximize the benefits of CF-ABS in FDM, process parameters should be carefully optimized. Key factors impacting the mechanical behaviour of printed objects include: Layer Thickness: lower layer thickness (e.g., 0.1–0.2 mm) will increase interlayer bonding, but also extend printing time.

Thicker layer will be reducing anisotropy, but can give rise to poor surface quality and material defects [39-42]. Raster Angle and Infill Density: Changing the direction of fibers at different angles also affects load path and stress distribution. The non-raster orientation yields tensile strength due to fiber alignment relative to load ( $0^\circ$ ) and balanced mechanical properties in other directions ( $\pm 45^\circ$ ). Higher infill densities ( $>50\%$ ) will increase the stiffness & strength of components, but at the same time expense of more material used and longer build time [43-45]. Temperature of the Nozzle and Printing Speed: Growth in the nozzle temperature induces flow of material and adhesive bonding between layers, which enhances interactions at interfaces. However, high temperatures can cause polymer matrix thermal degradation. For the printing speeds, being able to reach the ideal values is important since the trade-off between extrusion and mechanical performance can be maintained [46-48].

Because of the increasing industrial rising requirement for lightweight, high-performance and custom polymer composites, this study aims to present a holistic approach towards build orientation effects on mechanical characteristics (bending stiffness) to an FDM printed CF-ABS part. Tensile strength, flexural properties, and failure modes at two points were compared and show that this research offers vital criterion to optimize print settings in order to strengthen the material [49-52]. The outcomes will contribute to the broader area of additive manufacturing by addressing key questions related to anisotropic mechanical performance and fiber alignment, fostering

the adoption of CF-ABS composites for structural applications. This paper is prepared as follows: In Section 3, materials and methods utilized in this investigation will be detailed, including the investigational set-up and test method. Section 4 boons the results and discussion, focusing on the key results and their suggestions. Finally, Section 5 closes the paper with a summary of the main findings. The purposes of the current study stand:

- To experimentally investigate the tensile behaviour of FDM-printed ABS and CF-ABS components.
- To estimate the result of build orientation on tensile strength and deformation characteristics.
- To provide a through comparison between ABS and CF-ABS under identical printing conditions.
- To offer practical recommendations for material and orientation selection in structural FDM applications.

## 1.1 RESEARCH GAP

Existing publications on FDM-printed ABS and carbon-filled ABS mainly concentrate on individual impacts of process variables, for example infill density, raster angle or extrusion temperature. However, systematic comparative analyses in relation to the orientation-dependent tensile behavior of neat ABS vs CF-ABS under a controlled DOE-based environment are limited. On the other hand, most studies routinely reported lack of consistent experimental procedures where anisotropy in build direction is correlated with statistically validated mechanical response.

## 1.2 NOVEL CONTRIBUTIONS OF THE PRESENT STUDY

In light of the aforementioned limitations, this effort provides a methodical examination on the orientation-dependent tensile characterization of FDM-printed ABS and CF-ABS parts with controlled processing conditions. The principal novel contributions of this work are mentioned below:

- A comparison study on tensile specimens of ABS and CF-ABS prepared under the same FDM process parameters.
- An in-depth analysis regarding the effects of build orientation (X, Y and Z) upon the modulus, strength and ductility.
- Design of experiments (DOE) to statistically assess the relative importance of material type and build orientation.
- Provision of practical design-based guidelines based on the choice of building orientations for load-carrying polymer and composite parts fabricated by FDM.

The findings of this study would be helpful for improved understanding of anisotropic mechanical behavior in polymer composites FDM printing and provide useful suggestions for the selection of optimal build orientation in engineering applications.

## II. LITERATURE REVIEW

Additive Manufacturing (AM), mostly Fused Deposition Modeling (FDM), has developed polymer processing, where Acrylonitrile Butadiene Styrene (ABS) is a broadly used thermoplastic because of its cost efficiency, impact resistance and manufacturing simplicity [1]. However, neat ABS also has inherent disadvantages like poor interlayer adhesion, warping and moderate tensile strength which make it unsuitable in structural application [2]. These problems arise due to the layer-wise deposition method, which results in anisotropy and weak interlayer binding [3]. In order to overcome these limitations, Carbon Fibre-Reinforced ABS (CF-ABS) material has been established by combining short carbon fibers (CFs) into the matrix of the ABS [4]. Such reinforcement significantly improves tensile strength and rigidity, reduced warping [5].

Carbon fibers (CFs) have been used to improve interlayer adhesion, decrease anisotropic properties of the filaments of a polymer in terms of participating in matrix composites and making composite [6] applications like; aerospace, automotive and medical devices industry. Mechanical properties of CF-ABS are strongly reliant upon the fiber content, distribution and interfacial adhesion [7]. It has been demonstrated by studies that an optimal concentration of CF (5–15 wt. %) provides a combination of strength and ductility and any further increase in the fiber content would contribute to the brittleness [8]. Good fiber orientation in compounding results in an increase in load-carrying capacity and poor dispersion may produce voids, decreasing mechanical properties [9].

Surface treatments such as acid etching and coupling agents improve fiber-matrix adhesion, which reduces fiber pull-out during loading [10]. FDM printed parts exhibit anisotropic nature due to the cascade deposition, resulting in significant variation in mechanical properties depending on printing direction [11] X-Direction (Flat orientation): Layers are stacked perpendicular to load direction Enhanced tensile strength and ductility owing to continuous stacking of filaments [12]. Y-Orientation (Edge Build): It offers better tensile and flexural strength due to improved fiber orientation and load transfer [13]. Z-Orientation (Building Up): Shows the worst mechanical properties due to poor bonding between layers, leading to delamination under load [14]. According to the research, Y-aligned CF-ABS specimens show higher strength, while Z-aligned samples suffer from layer-to-layer adhesion problems and void occurrences [15].

The mechanical performance of CF-ABS depends significantly on FDM processing parameters which require careful tuning [16]: thinner layer height (0.1–0.2 mm) increases interlayer adhesion but also lengthens the printing time, whereas thicker layers lead to a worse structural integrity [17]. Complementary heating plates can reduce warping and increase interlayer adhesion and strength [18]. A 0° screen angle maximizes the tensile strength for fibers aligned with the direction of load [19]. ±45° raster angles provide the maximum shear strength which makes them suitable for impact resistant applications [20]. Higher infill densities yield higher stiffnesses while also increasing material usage; 80% is an optimal compromise [21]. Hotter nozzle temperature result on better interlayer bonding while it introduces danger of thermal degradation to the polymer matrix [22].

The optimal speed for printing (50–75 mm/s) is a trade-off between mechanical operation and printing rate [23]. The anisotropic nature of FDM printed with CF-ABS leads to specific failure modes [24] Delamination: This is the dominating mode in Z oriented prints due to low interlayer adhesion as in [25]. Fiber Pull-Out: Occurs when interfacial strength between the fiber and matrix is weak, which reduces reinforcing effects [26]. Matrix Crack: Composites with high fiber content were reported as brittle [27]. Shear-Induced Degradation: commonly observed at ±45° raster directions that leads to slow decay instead of catastrophic failure [28].

Few works differentiate between CF-ABS and other reinforced polymers: PC- ABS versus CF-ABS: Polycarbonate ABS (PC-ABS) outperform CF-TPE in tensile strength as well as flexural strength, especially at higher infill density [29]. ABS/TPU Blends: Up to 20 wt. % of thermoplastic polyurethane (TPU) could be blended. % improves the interlayer bond but with no loss in yield strength [30]. Hybrids: Glass fibers (GF), graphene oxide fillers can be added to enhance thermal stability and mechanical properties of CF-ABS [31]. Although many successes have been achieved, several challenges still remain: The research on the hybrid CF-ABS/glass fibers, CNTs or Kevlar fiber-based composites is very scarce [32]. ABS/CF/GF hybrid composites are reported to possess improved wear resistance and thermal stability [33].

The techniques of AIML related to optimization FDM parameters are less mature [34]. Predictive modeling may accelerate the process of material properties optimization [35]. Most of works concentrate on static mechanical behaviors, and little information about fatigue performance, creep resistance and environmental degradation has been presented [36]. Results of the accelerated aging indicate that ABS is more affected by UV and heat exposure than PLA [37]. The principal limitation of important FDM printing is the evenness of the bed temperature and the continuity of filament feed [38]. -The porosity of the recycled ABS is larger and this reduces the mechanical strength in spite of a minor molecular degradation [39]. -Wear: GF/ABS composites obtain the lowest wear rates, which makes it suitable for high-wear applications [40].

Electrical Conductivity: The vertical printed ABS/carbon black composite exhibits 40% less charge transfer resistance than the horizontal printed one, which is very advantageous to sensing [41]. Hybrid reinforcement (CF + GF + CNTs) for enhancement of multifunctional properties [43]. AI-based parameter tuning for improved mechanical properties [44]. Extended durability tested under mechanical, thermal, and environmental stresses [45]. Sustainable AM technologies, including recycled materials and low-energy printing [46]. CF-ABS composites have a significantly enhancing effect on the mechanical behavior of FDM-printed parts, which is also affected by the printing direction and process parameters. However, anisotropy, interfacial adhesion and long-term reliability are still problematic [47].

## II.1 INFILL ARCHITECTURE AND DENSITY

The tensile strength of FDM polymers and composites is strongly dependent on infill architecture and density. Seshaiha Turaka et al. modified infill from 20 to 80% at 0.32 mm layer height on a CreatBot F430, and they determined CF-ABS performance with an 80% infill density reached a tensile strength of 36.92 MPa, being the highest among other configurations (with a 64.74% higher flexural and a and also improved flexural and compressive performance linked with lower infill configurations. Moreover, honeycomb pattern also delivered high results [1]. Consistent with this, improving infill and the refined lattice (such as Tri-hexagonal) increased ABS UTS on Ultimaker machines [20]. In Stratasys machines, ABS-CF10 displayed a significantly improved tensile and flexural strength in relation to ABS-M30; for the CF level type, 80% sparse design presented the best performance at strength over weight rate [40].

## II.2 ORIENTATION-INDUCED ANISOTROPY

Build orientation significantly affects tensile and flexural performance in both ABS and CF-ABS due to anisotropic interlayer bonding. The horizontal (X) orientation provided the maximum tensile and flexural strength, followed by vertical (Z) orientation, which yielded the minimum; approximately twice as much amount of strain energy was absorbed in case of horizontal samples related to the vertical ones [4]. The tensile strength of ABS was reduced by 44.3% when changing the printing orientation from 0° to 90° (UP-Box) [9]. For CF filled systems, Z-strength of the CF-ABS was 47% lesser than the flat builds but stiffness increased by about ~90% with CF in the flat orientation [13]. In conventional FDM research, tensile properties of ABS parts relating to the injection-molded ABS were found as 65±72%, which are affected by rasters and air gap with the axial direction performing better among them [38].

## II.3 RASTER ANGLE, LAYER HEIGHT, AND GEOMETRY

Introduction The tensile strength and flexural resistance of SCFR-ABS decreased by 22% from 31.5 to 24.6 MPa and by 15%, respectively, with a raster orientation angle ranging from zero to 15 degrees; however, certain angles (e.g., 60°) promoted crack deflection for tougher specimens [23]. Integrity studies showed that 0/90° rasters outperform ±45° in tensile/fracture behavior in ABS/PLA settings [24]. ABS tensile strength increased by 33% at 0.1 mm/5 (0°) after improving the rasters of ABS with a chamber temperature higher to reduce voids and therefore improve strength [25]. 0° rasters, 0.8 mm nozzle, 0.15 mm layers achieved the least number of cracks development and the longest fatigue life time under thermo-mechanical stresses of ABS [26].

## II.4 INFLUENCE OF CARBON-FIBER REINFORCEMENT AND MATRIX SELECTION

This is because usually CF reinforcing will increase stiffness/strength and reduce ductility. 50% overall infill, hexagonal with 5–15 wt% CF At a load of 0.1 kg, hexagonal (CF-ABS) structure has reached a strength of 21.41 MPa (~24% higher than ABS) and the modulus equals to 1.47 GPa [3]. The tensile strength of the 13 wt% CF filled sample (CF-ABS) was about 30% that of ABS; a 50% infill often led to significant enhancements [8]. For flexural tests, it was reported that CF-ABS had a 58.7% increase in modulus compared to ABS with P450 orientations outperforming P0 and ±45° [14]. It is crucial to select an appropriate thermoplastic matrix: The tensile strength of CF-PA6 was roughly 68% higher than that for CF-ABS, whilst the latter's modulus was about 106% greater than that of CF-PA6; the thermal degradation onset temperature for CF-ABS exceeded 270 °C [43-54]

## II.5 PROCESS-ASSISTED STRATEGIES AND NANO-MODIFICATION

Anisotropy can be reduced by help in processing. Additional heating at 160 °C could boost the strength under tension of CF/ABS by 31% and enhance the ductility by a factor of 439%, while reducing warpage from 12.3 mm to as low as 1.7 mm at a full infill density [27].

In high-temperature composites, a tensile strength was achieved by CF/PEEK of 94 MPa at 440 °C nozzle and 280 °C bed temperatures, where low thickness layers combined with a slow speed induced high interlayer adhesion [30]. Nano-fillers and additives also help with the mechanical properties: 2 wt% graphene oxide in ABS increased tensile strength and modulus, but decreased elongation (5.8% to 2.9%) [32]. 10–20% v/v fine expanded-perlite fillers ( $\leq 90 \mu\text{m}$ ), maintained ABS UTS near 21.7 MPa; coarse/more load reduced strength because pore and layer dislocation [37]. ABS+CNT outperformed ABS+CF in tensile strength in some cases (34.18 vs. 27.25 MPa) while a lower layer thickness improved the property by reducing the porosity [55-57]

## II.6 MICROSTRUCTURE, VOIDS, RECYCLING, AND SCALE

Reducing the pore size improves the interfaces: roller-pressed LAAM CF-ABS (13 wt% CF) reduced micro void volume from 14.0% to 10.0% and improved interlaminar adhesion [36]. Recycling was found to have increased porosity ( $\approx 11\% \rightarrow 17\%$ ) which caused in a 10% reduction in the stretchy strength of ABS and 25% reduction in strain at break (5.2%  $\rightarrow$  3.9%) [39]. Nylon-12 CF (Fortus 900mc) achieved a UTS of 97.41 MPa for side orientation, but only 22.63 MPa in the upright position; solid infill improved strength at the expense of ductility [41]. Multi-function, multi-material printing magnifies the practical concerns (ensuring even bed heating and feed control) that must be resolved before mechanical improvement [42]. Porosity and tensile strength increased because recycling resulted in molecular degradation and void formation [47], [48]. The large-area AM process also suffers from thermal gradient, filament feeding instability and void defect [49], [50].

## II.7 ARCHITECTED LATTICES AND STRENGTH-DUCTILITY TRADE-OFFS

Hierarchical honeycombs of ABS, CF-ABS (CF 15%) and CNT-ABS indicated that the compressive load was maximized for CF-ABS honeycomb's structure (924.63 N) and second order hierarchies improve stiffness [1-3]. Across several studies, factors including orientation (flat/side), raster alignment, minimum layer thickness, careful temperature control and higher but effective infill in addition to CF/CNT reinforcement collectively improve strength and stiffness – although ductility frequently decreases – with Z-direction failures again primarily dictated by poor interlayer bonding [4-8].

Despite comprehensive parameter studies, there is a dearth of DOE-directed orientation-specific tensile characterization of CF-ABS that (i) holds non-orientation parameters constant, and (ii) provides a full mechanical suite (UTS, yield strength, modulus, ductility, breaking stress) to quantify the strength-ductility trade-off for design considerations [9-13]. Previous studies involving changes of parameters (infill/raster/temperature) with orientation combined, thus obfuscating the origin of effects or focusing on non-tensile tests (compression/impact) or other matrix/geometries PA6, PEEK [14-20]. Focuses on build orientation (X/Y/Z) and material type (ABS vs CF-ABS) under constant process parameters, utilizes a Taguchi-based DOE for factor precedence, and showcases the influence of factors on performance by tweaking only one mechanical factor at a time.

Orientation specific values such as UTS, modulus, yield, break strength and ductility are provided in this analysis [21-26]. The results indicate when CF-ABS provides useful functionality (e.g., CF-ABS-X maximum UTS) and when regular ABS may be more appropriate due to ductility requirements, which provide some general guidelines for selecting between load-bearing and compliance-focused FDM parts [27-32]. The focus of this data-driven but concentrated orientation study addresses the identified gap and provides design-ready recommendations in a short-term horizon for polymer composite FDM. Hierarchical lattice designs and honeycomb infill patterns contribute towards the improvement of their compressive strength, stiffness along with energy absorption behaviour [51-54]. In order to address the identified research gap, this study employs a a DOE framework based on the Taguchi method in fine-tuning the impact of build orientations (X, Y, Z) and material types (ABS vs. CF-ABS) on tensile behavior.

All of the other printing settings – such as infill percentage, raster angle, nozzle temperature, print speed, and layer depth – were kept constant to isolate the effects of build orientation and material type. ASTM D638-type tensile samples were made-up using a Creality K1C industrial FDM printer, and mechanical testing was led using a digital uniaxial tensile testing machine. The mechanical properties (UTS, yield stress, break strength, Young's modulus and ductility) were analyzed using a statistics approach. The method enables that mechanical differences can be assigned reliably to orientation and reinforcement effects, in a reproducible and clear manner. CF reinforcement generally improves stiffness and load-bearing capacity but often reduces ductility [58-62]

## II.8 SUMMARY OF LITERATURE

Build direction is well known to be an important influencing factor of the tensile properties for FDM-printed polymer components. In common, X- and Y-oriented samples are stronger and stiffer in tensile compared with Z-orientation due to the more level bonding within layer and decreasing interlayer failure [3], [9]. The anisotropic behaviour is largely owing to the layer-wise deposition process and poor inter-diffusion of molecules between adjacent layers [23]. However, the majority of published studies are based on a specific material system and there is little available work in comparing directly under same processing and material control. The tensile stiffness and load capacity of the composites containing CF-ABS have been enhanced, but issues related to adequate blending between fibre and matrix, formation of voids, anisotropy due to orientation continue to be critical [24], [30].

Most of the literature have addressed on filament/material approach while to date integrating of build orientation effect with CF reinforcement in tensile performance is scarce. Recently, some research activities have been observed to focus on enhancing interlayer adhesion, reducing anisotropy and multi-functional performance of FDM composites [57], [63], as well as developing AI/ML techniques for parameter prediction and optimization [64], [65] in addition to pursuing sustainable approaches including use of recycled polymers and eco-friendly composite manufacturing [58], [59]. Finite element analysis has also been employed to simulate stress and strain in FDM parts yet the available experimental-numerical correlation for CF-ABS systems under common tensile loading is inadequate [60-62], hence the capability to develop accurate predictive models of orientation-sensitive composite components is limited.

Table 1: Comparison of Existing Studies on Orientation/Parameter-Dependent Tensile Behaviour of FDM Printed ABS and CF-ABS.

Study	Material	Orientation considered	DOE used	Constant parameters	Key findings	How present study differs
Seshaiah Turaka et al. (2024) [1]	ABS, CF-ABS (Think Robotics, India)	Not explicitly (focus: infill density)	No (parametric study)	Yes (nozzle temp., speed, layer thickness fixed; infill varied)	CF-ABS at 80% infill showed 36.92 MPa tensile strength; higher infill + CF improves properties	Present work compares build orientations (X/Y/Z) for ABS & CF-ABS under controlled conditions instead of only infill variation
Vigneshwaran Karupaiah et al. (2022) [3]	ABS / CF-ABS (Nanovia, France; SCF 5–15 wt%)	Yes (reported best in Y-orientation)	No (multi-parameter comparison)	Partially (multiple infill patterns & densities varied)	CF-ABS with hexagonal + 50% infill → 21.41 MPa UTS, modulus 1.47 GPa	Present study gives direct ABS vs CF-ABS orientation benchmarking with consistent printing plan and experimental tensile testing
Anubhav et al. (2023) [4]	ABS+ P430	Yes (X vs Z)	No	Yes (100% infill; fixed layer thickness & temps)	Horizontal (X) highest strength; Vertical (Z) weakest; orientation dominates	Present study extends to two materials (ABS & CF-ABS) and reports full orientation response including stiffness and failure behaviour
Abdul Quader Shurjeel et al. (2021) [6]	CF-ABS / PC-ABS	Not explicitly	No	Partially (infill & raster varied)	0° raster and higher infill improve strength; PC-ABS > CF-ABS	Present work isolates build orientation effect (X/Y/Z) rather than raster angle/infill combinations
Olusanmi Adeniran et al. (2022) [8]	CF-ABS, CF-PA (15% CF)	Not specified	No	No (printing temperature varied)	CF-PA6 shows ~68% higher strength vs CF-ABS; CF-ABS higher modulus	Present study focuses on orientation-based anisotropy in ABS and CF-ABS (not matrix comparisons like PA)
E. A. Syaefudin et al. (2023) [9]	ABS / PLA	Yes (0°, 45°, 90°)	No	Yes (layer thickness fixed)	ABS tensile strength reduced 44.3% from 0° to 90°	Present work provides material reinforcement comparison (ABS vs CF-ABS) plus full tensile response with orientation mapping
J. Yan et al. (2023) [13]	ABS/CF-ABS, PLA/CF-PLA, PA & PETG composites	Yes (F vs Z)	No	Yes (temp/thickness fixed)	CF-ABS shows ~47% lower Z strength than F-direction; stiffness improved ~90% in F	Present study gives experimentally validated orientation ranking for ABS & CF-ABS using tensile coupons and constant settings
Kui Wang et al. (2019) [14]	ABS, CF-ABS, KF-ABS	Yes (0/90 vs ±45; horizontal vs side)	No	Partially	CF-ABS modulus increased 58.7% over ABS; orientation/raster affect flexural	Present work specifically benchmarks tensile UTS & stiffness across orientations for ABS and CF-ABS specimens
Chamil Abeykoon et al. (2020) [35]	ABS, CFR-ABS, CNT-ABS etc.	Yes (raster orientation 0°–90°)	Yes (optimization)	No (multiple factors varied)	Infill density + raster orientation significantly affect tensile strength	Present work is simpler + targeted: only ABS & CF-ABS with orientation-dominant tensile investigation, suitable for manufacturing design
S.-H. Ahn et al. (2002) [38]	ABS P400	Yes	No	No	Tensile strength depends on raster orientation/air gap; FDM ABS ~65–72% of injection molded	understanding to CF-ABS filament composite and produces orientation-dependent tensile benchmarks relevant to current low-cost FDM platforms

Source: Authors, (2026).



### III. MATERIAL AND METHODS

Systematic experimentation was employed in this work to explore in what way build direction moves the tensile properties of FDM-printed ABS and carbon fiber-reinforced ABS (CF-ABS) parts. In order to obtain reproducible results, all samples were fabricated under controlled processing conditions, and tensile tests performed according to ASTM standards. Material type and build orientation effect was statistically evaluated using a structured Design of Experiments (DOE) methodology.

#### III.1 MATERIAL SELECTION

Fused deposition modeling (FDM) is utmost current additive manufacturing processes used to fabricate polymer parts, known for its low cost, simplicity and ability to produce complex objects with no material loss. This paper studies the tensile stress mechanical properties of Acrylonitrile Butadiene Styrene (ABS) and CF-ABS, in different orientations. The materials used in this learning were solid space filaments of nominal diameter 1.75 mm. The material properties, delivered by the manufacturer, are given in Table 2.

Table 2: Technical features of the filaments material made of ABS and CF-ABS.

Property		
Material	ABS	CF-ABS (carbon fiber reinforced ABS)
Filament Diameter	1.75 mm	1.75 mm
Colour	White	Black
Density (g/cm <sup>3</sup> )	1.05	1.11
Poisson's Ratio ( $\nu$ )	0.36-0.38	~0.35–0.40
Modulus of Elasticity (E) (GPa)	2.62	5.21
Flexural modulus (GPa)	2	5.26
Ultimate Tensile Strength (UTS) (MPa)	47.0	46.0
Heat Deflection Temperature (°C)	90	76
Tensile strength		
At yield	47 MPa	36.8 MPa
At break	34 MPa	46 MPa

Source: [66], [67].

Note that the carbon fiber filament reinforcement was not manually added by us but rather it was already present within the original CF-ABS supplied through vendor. The CF-ABS is a short carbon fiber-reinforced thermoplastic composite filament and the carbon fibers are well-dispersed in the ABS matrix during the extrusion of the filament [52], [63]. Thus, the reinforcing found in 3DP follows from the natural composite character of the filament and not a result of transferring reinforcement or adding continuous fibers to FDM process [64, 65]. This method offers enhanced stiffness and strength, but can still be used with standard FDM printing systems in the same processing conditions [58-62].

#### III.2 PRINTING PARAMETERS AND EQUIPMENT

Samples were fabricated using the Creality K1C industrial FDM printer, known for its accuracy, repeatability and wide range of applicable materials. Printing settings were kept consistent for all printed parts to provide uniformity. Table 3 presents the standardized development limits followed in the present study during the production of the specimens with the Creality K1C industrial grade FDM printer. A 100% infill was used to ensure fully dense samples and minimise internal porosity. The nozzle size is 0.4 mm and the deposit height is also set as 0.2 mm to balance between printing quality and printing speed. For high resolution prints, a print speed of 120 mm/s was maintained; as the optimum compromise between accuracy and construction time. The extrusion temperature was set at 245 °C to achieve sufficient filament flow and adhesion. This temperature was built on the manufacturer's recommended processing window for ABS and CF-ABS filaments, to provide optimum viscosity and uniformity of layer adhesion.

This temperature enables correct polymer chain hopping between adjacent layers, thus decreasing interfacial voids and the force of adhesion. Former researches reported that extrusion at temperatures ranging about 240–250 °C is the temperature to use for achieving a proper fit between stabilization of stable flow and prevention of high-temperature degradation, for ABS based composites. Therefore, a default temperature of 245 °C was defined to guarantee the same reliable and perfect print quality for all test prints with always a nozzle temperature at 215 °C ensuring good extrusion. To increase adhesion of the first layer and prevent warping, a hotbed temperature of 105°C was used. Cubic infill pattern selected for its strength and uniform distribution of the load. In addition, a cooling rate of 100% was used to regulate the solidification process and improve the bonding quality between layers. These settings were applied consistently on all builds to ensure consistency/reliability of the experimental results.

Table 3: Printing Parameters.

Process Parameters while printing Build orientation	
Infill density	100%
Nozzle Diameter (mm)	0.4
Layer height (mm)	0.2
Print speed (mm/s)	120
Extrusion Temperature	245 °C
Infill pattern	Cubic
Bed temp	105 °C
Cooling speed	100%

Source: Authors, (2026).



Figure 1: Creality K1C industrial-grade FDM printer used for specimen fabrication.

Source: [66].

The industrial-type FDM printer, Creality K1C used in this study is shown in Figure 1. Its exact construction and dual-gear mechanism ensured uniform extrusion quality for ABS as well as CF-ABS samples. The trials were conducted using a Creality K1C industrial-grade FDM printer with dual-gear direct driver extruder. All the specifications for the printer are given in Table 4. To ensure efficiency and dimensional precision, a quick printing method was used. The selected process parameters were based on a substantial review of prior studies and preliminary experiments to ensure optimization for the tensile properties of printed samples.

Table 4: FDM Printer specification.

Printing Technology	Fused deposition modeling
Build Volume	220x220x250mm
Product Dimensions	355x355x482mm
Printing Speed	≤600mm/s
Acceleration	≤20000mm/s <sup>2</sup>
Printing Accuracy	100±0.1mm
Build Plate	PEI flexible build plate
Printable File Format	G-Code
Layer Height	0.1-0.35mm
Extruder	Dual-gear direct drive extruder
Filament Diameter	1.75mm
Nozzle Diameter	0.4mm
Nozzle Temperature	≤300°C
Heat bed Temperature	≤100°C
Supported Filaments	ABS, PLA, PETG, PET, TPU, PA, ABS, ASA, PC, PLA-CF, PA-CF, PET-CF
Slicing Software	Creality Print, Cura 5.0 and later version

Source: [66].

### III.3 INFILL DENSITY

The infill density was set to be 100 percentage for all samples, in order to ensure the fully dense properties of components and thus minimize the internal porosities as well as maximize the mechanical strength. This is in accordance with previous findings, where infill

density has a momentous effect on tensile properties of the structure as the fully dense ones result in enhanced load carrying capacity and uniform stress distribution.

**III.4 INFILL PATTERN**

A cubed infill pattern was selected due to significantly better isotropic properties and ideal load distribution versus other infill types. Previous research studies showed that stiffened cubic infill patterns possess better stiffness and strength with reasonable material usage.

**III.5 PRINTING SPEED**

The printing speed was determined at 120 mm/s based on the capacity of the printer and previous criteria of FDM-printed polymer composites. The lifting speed accelerates the printing but may cause a worse layer adhesion and surface finish. The speed selected achieved a balance between the production efficiency and the mechanical reliability.

**III.6 LAYER HEIGHT**

The layer height of 0.2 mm was chosen to enhance mechanical properties and surface finish. Previous studies indicate that a lesser deposit height results in better interlayer adhesion and tensile strength due to the more effective molecular diffusion and bonding between layers.

**III.7 BUILD ORIENTATIONS**

The building direction is an important consideration for the mechanical properties of FDM printed parts since AM processes are usually anisotropic. Three characteristic orientations of build, presented in Figure 2 were evaluated: X-Orientation (Flat): The layers are oriented perpendicular to the loading direction. Y-Orientation (Edge): Layers are oriented perpendicular to the load direction but still in-plane. Z-Orientation (Standing): The layers are arranged perpendicular to the loading direction and the interlayer bonding is the principal means of support. Furthermore, previous research results indicated that the tensile property of Y-oriented samples is supposed to be optimal due to the better order of layer bonding and stress distribution while Z-oriented was expected worse tensile strength because of relatively low interlayer adhesion. The X, Y and Z construction orientations are illustrated visually in Figure 2. These orientational factors have a large influence on layering and the interfacial adhesion that determines the anisotropy of tensile properties.

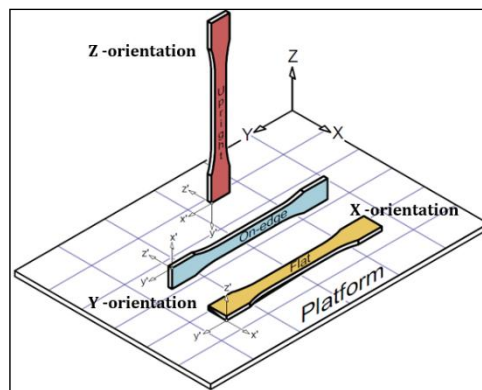


Figure 2: Diagram representation of the three Build orientations studied.

Source: [68].

**III.8 DOE**

An orthogonal array-based experimental (OAE) procedure was employed in order to systematically determine the effect of build orientation and material type on tensile strength of FDM printed specimens. The Taguchi method is a useful, statistically-based tool for minimizing the number of actual experiments required at a research stage and maximizing what one can learn about factor effects. In this study, two primary control factors were considered (A) Build Orientation with 3 levels (X-Y-Z), and (B) Material Type with 2 levels (ABS-CF-ABS). A L6 orthogonal array was selected, taking these factors into account, and all levels were equally represented only in six different trials. All trials were repeated 3 times to increase reliability and reduce random error.

The DOE meant to evaluate the result of build orientation and material type on key mechanical responses: Ultimate Tensile Strength (UTS), Yield Stress (σ<sub>y</sub>), Break Strength σ<sub>b</sub>, Ductility ε<sub>b</sub>, Young’s Modulus E. Signal-to-noise (S/N) ratio is a quality evaluation/criterion in the Taguchi method to quantify variability and robustness. For the properties requiring higher values (UTS, E), using the larger-the-better criterion, as in where S is defined mathematically by:

Taguchi Signal-to-Noise (S/N) Ratio – “Larger-the-Better” criterion Equation

$$S/N = -10 \log_{10} \left( \frac{1}{n} \sum_{i=1}^n \frac{1}{y_i^2} \right) \tag{1}$$

Where:

- S/N = Signal-to-Noise ratio (dB)
- n = Number of experimental repetitions
- $y_i$  = Measured response value for the  $i^{th}$  trial (e.g., tensile strength, Young’s modulus)
- i = Trial index (i = 1, 2, ..., n)

This “larger-is-better” criterion is used when the objective is to maximize the response, such as ultimate tensile strength or elastic modulus. Where n is the quantity of runs then  $y_1, y_2, y_n$  are the response. The averages of the levels were then computed and trend analysis was performed, main-effect and interaction diagrams plotted to provide an evaluation of the features' influence on mechanical properties. The "larger-is-better" expression (Eq. 1) enables that better mechanical properties correspond to higher SN ratios, indicating good system parameters. To further analyze the effect of each factor, this study performed Analysis of Variance (ANOVA). The pure effect of each factor on the overall variance (in the response) was estimated using the following relation Percentage Contribution of Factors (ANOVA) Equation

$$P_i = \frac{SS_i}{SS_T} \times 100 \tag{2}$$

Where:

- $P_i$  = Percentage contribution of the  $i^{th}$  factor (%)
- $SS_i$  = Sum of squares of the  $i^{th}$  factor
- $SS_T$  = Total sum of squares

This equation quantifies the relative influence of each control factor on the overall variation of the response. Where  $P_i$  is the percent contribution of  $i^{th}$  factor,  $SS_i$  is sum of square for each such factor and  $SS_T$  is total sum of squares. These analyses indicated the key parameters with regard to tensile strength and modulus. The best combination of parameters that ensured the maximized strength and stiffness with minimum variability were calculated from S/N ratio and ANOVA analysis. As a consequence, the DOE framework delivered a systematic and statistically supported analysis procedure for optimizing FDM process parameters.

An L6 Taguchi array was used to study the orthogonal independent and interactive effects of two factors: material (ABS, CF-ABS) and build orientation (X, Y, Z). This procedure provided a clear view how each factor influences process performance. Each combination of factors was evaluated in triplicate to ensure statistical soundness, resulting in 18 tensile test samples (9 ABS and 9 CF-ABS). The response was characterized by tensile properties such as extreme load (N), ultimate tensile strength (MPa), percentage extension, break strength (MPa), yield stress (MPa) and Young’s Modulus (MPa).

A Taguchi orthogonal array was working to reduce the number of experiments, but retain statistical power. The factors that were considered are; Factor A: Build orientation – (3 levels, X, Y and Z) Factor B Material type (2 levels, ABS and CF-ABS). An array L6 model was developed which resulted in six experimental conditions. All conditions were performed in triplicate creating six tensile samples. The analysis of S/N ratio was carried out under a “larger-is-better” criteria to find the finest level of parameters for determined value of tensile strength and modulus.

Table 5: Layout of L6 Array.

Run	Factor A – Orientation	Factor B – Material
1	X	ABS
2	Y	ABS
3	Z	ABS
4	X	CF-ABS
5	Y	CF-ABS
6	Z	CF-ABS

Source: Authors, (2026).

It was a deliberate choice to use only two factors for the DOE with tensile response since such measures limit the influence of orientation and type of material. This method simplifies the experimental complexity and provides a statistically meaningful correlation to anisotropy effects.

### III.8.1 Experimental Factors and Levels

The experimental design was intended to explore the mutual effects of build orientation and material content on tensile strength. Two control variables were selected because they significantly influence the mechanical performance of FDM.

Table 6: Factors & Levels.

Factor	Symbol	Levels	Description
Build Orientation	A	3	X (Flat), Y (Edge), Z (Vertical)
Material Type	B	2	ABS, CF-ABS

Source: Authors, (2026).

All possible combinations of factors were evaluated for three replicates leading to 18 experimental runs (6 combinations  $\times$  3 repeats). One of the orthogonal arrays L6 was selected, it effectively handles two factors at three levels and reduces the number of experimental runs. This design guarantees statistical balance and yields sensitivity to a main effect without confounding.

### III.8.2 Response Variables and Evaluation Criteria

The response variables selected were:

- Ultimate Tensile Strength (UTS, MPa)
- Yield Stress ( $\sigma_y$ , MPa),
- Break Strength ( $\sigma_b$ , MPa),
- Ductility ( $\epsilon_b$ , %),
- Young's Modulus (E, MPa).

The Taguchi signal/noise (S/N) ratio technique and an ANOVA were used to analyze these responses for the identification of significant parameters and optimal conditions. For UTS and E, the larger the better criterion was rummage-sale and mean effect plots were used to analyse factor sensitivity for all other responses.

The Taguchi analysis workflow included:

- a) Factor combinations from the L6 array.
- b) Performing 3 replicates per condition to reduce experimental error.
- c) Computing S/N ratios using Eq. (1) and identifying the important factors according to Eq. (2).
- d) Graphing main and interaction effects for UTS, yield stress, and modulus to represent orientation-material interactions.

By this systematic approach, it was ensured that both material-type and orientation-effects were statistically verified which resulted in a comprehensive and reproducible conclusion about the tensile behavior of FDM reproduced composites. The use of DOE approach added a significant scientific value to this research. With the use of a Taguchi L6 orthogonal array, the study was efficient in determining individual and collaborating effects of build orientations and materials on tensile behaviour with minimal number of experiments executed. This factorial design verified that observed changes in tensile strength, modulus and elongation were statistically attributed to process variables rather than random error.

Objective ranking of the significance level of the parameters was carried out using S/N ratio and ANOVA estimations, and build orientation was found as most influencing parameter for mechanical variation closely followed by material type. Accordingly, the DOE procedure has enhanced peak strength and stiffness parameterization but also increased reproducibility and confidence concerning experimental results. The results obtained through this systematic framework confirmed the identification of an optimal print orientation-material combination in achieving improved mechanical properties in FDM-printed composite materials.

### III.9 FABRICATION OF 3D PRINTING SPECIMEN

The tensile test specimens were designed built on ASTM D638 via SolidWorks. The 3D models were then converted into .STL file processed set-up which is often used for 3D printing and readable by slicing software. Slicing was performed on ORCA Slicer v2. 2. 0 with key process variables fixed to secure repeatability of production. The settings of the process were set as: Infill Density: 100%, Printing Speed: 120 mm/s, Layer Thickness: 0.2 mm, Infill Pattern: Cubic and Nozzle Diameter: 0.4mm. The STLs were added to the slicer, and for each part of build orientations were changed from X, Y onto Z axis to study how the parts behave mechanically. The slicing process also generated useful data such as nozzle position, weight to be expected for the object, desired length of filament and duration to print. Upon verifying these parameters, the finished files were exported and saved as G-code files.

3D printer Instructions were transferred to 3D printer through USB drive. 3D printing machine, dual-nozzle 3D printer was first fed with ABS or CF-ABS filaments, and then FDM (Fused Deposition Modeling) printing procedure was adopted. Each sample was printed as an individual data point to maintain consistency and avoid batch-to-batch effects of printing. The automatic printing system ensured uniformity of all the samples. Nine samples were generated using ABS and 9 samples using CF-ABS producing a total of 18 extracted tensile specimens. Three specimens per orientation (X, Y and Z) were printed for making comparisons. Once printing was complete, the samples were detached carefully from the print bed. If support were present, these were manually removed for accuracy in dimension. Each sample was later checked to confirm that it complied with the ASTM D638 typical dimensions. After that, the specimens were coded for tracking and prepared for subsequent tensile test.

### III.10 TENSILE TESTING PROCEDURE

Tensile testing was done in accord with ASTM D638 that measures fracture behavior of an applied load, within its gauge lengths of the sample. Test method followed ASTM D638, which measured the tensile strength and elongation of a material. This process is commonly applied for woven, non-woven and felted structures however modified to be used as a technique for tensile testing of FDM-printed ABS and CF-ABS samples. Dimensions of the sample, such as gauge width and thickness, were measured with a micrometer prior to testing. A 25 mm length were marked for each sample. The acquisition signals were transferred into the tensile testing software in directive to ensure accurate stress-strain conversion.

Tensile testing was conducted using a uniaxial digital tensile testing machine (Shanta Engineering, Model: SET-T-20kN) at tension mode. The samples were clamped tightly with fixed and moveable clamps. The lower grip was fixed and the upper one had moved at a continuous crosshead speed of 10 mm/min until the sample failed. After fracture, the fractured sample was removed from the grips and its elongation measurements were obtained using vernier's caliper. The tensile testing system recorded and analyzed several mechanical properties including Ultimate tensile stress (MPa), Load at break (N), Elongation at peak (mm), Elongation at break (mm), Break strength (MPa), Percentage elongation at maximum load and NBS, Final dimensions of films (width, thickness, length in mm or cm); The final cross-sectional area of the test specimen (mm<sup>2</sup>); Yield stress (Mpa);,Yield load (.N),Load-displacement curve.

Following the completion of testing, a representative tensile stress–strain curve was developed in the software to indicate the mechanical behavior of both ABS and CF-ABS under tensile loading. The recorded data were stored as a PDF for further analysis. This method of tensile characterization enables the repeatability and reliability for mechanical property assessment of FDM-printed ABS and CF-ABS materials under uniaxial tensile loading. The uniaxial digital tensile testing machine used for characterization of the mechanical properties of FDM-printed ABS and CF-ABS samples are given in Table 7. The equipment, manufactured by Shanta Engineering (Model: SET-T-20kN), operates between the modes of tension, and has a maximum load of 2000 kg suitable for strong materials.

Table 7: Tensile Strength Machine Specification.



Name	Uniaxial testing machine digital type testing machine
Make	Shanta Engineering
Model	SET-T-20kN
Max. capacity (Kg)	2000
Digital Panel	In build digital display with machine
Load Cell 1	1 kN
Load Cell 2	20 kN
Max. crosshead displacement without grips/fixtures (mm)	900
Displacement resolution (mm)	0.2
Column clearance(mm)	450
Machine Dimensions w × d × h in (mm)	1100 × 400 × 1800

Source: [66]

The testing machine is equipped with a digital display screen, which allows the user to easily see load displacement values, and accurate configuration test result in time. It offers two load cells—1 kN and 20 kN—ensuring that a large number of force applications can be carried out with high accuracy. Without grips and holders, this machine can accept specimens of varying size up to 900mm crosshead travel. For higher measurement precision, the system provides a displacement resolution of 0.2mm. Clearance of 450 mm between the columns allows enough space to align specimens and attach grips. The size (1100 mm × 400 mm × 1800 mm) of the machine can maintain test environment stable and reduce disturbance outside. This criterion collectively improved the accuracy, repeatability and reliability of tensile testing process which aids in determining mechanical properties for ABS and CF-ABS specimens under uniaxial tensile loadings

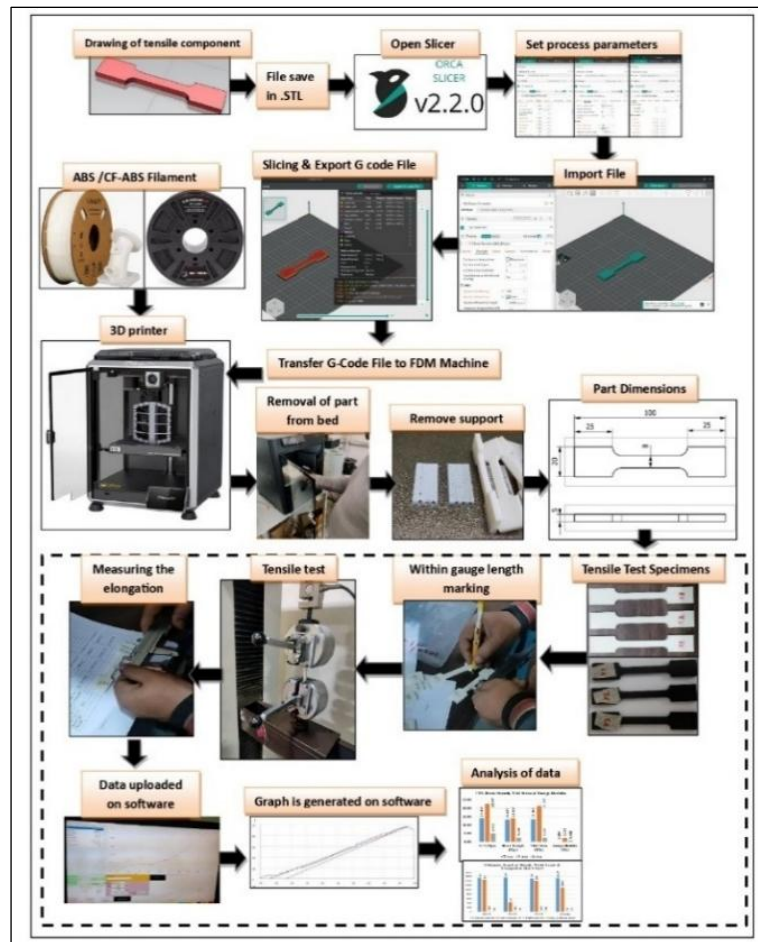


Figure 3: Flowchart of specimen preparation and tensile test with uniaxial digital tensile machine. Source: Authors, (2026).

As exemplified in Figure 3, the procedure consisted of 3D printing, post-processing and tensile tests by means of digital uniaxial machine (20 kN) test. Numerical calculations displayed sequentially ( $\text{Stress} = 545.7 / 40 = 13.6425 \text{ MPa}$ ,  $\text{Strain} = 0.753 / 25 = 0.03013$ , etc.). The applied force during loading was directly recorded from the uniaxial testing machine. The cross-sectional area was measured for accuracy with a micrometer, prior to testing. The stress is of crucial importance because it has direct effect on the material selection and mechanical performance estimation.

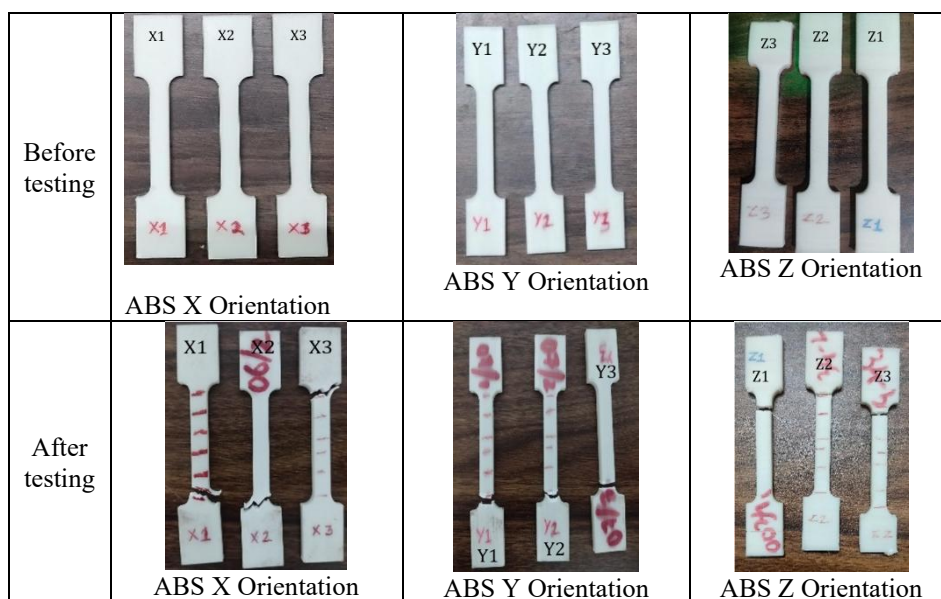


Figure 4: Tensile ABS samples at X, Y, and Z directions before and after tensile testing; reveals failure modes depended on orientation. Source: Authors, (2026).

In Figure 4, differences in the failure of ABS samples are highlighted. ABS-Y displayed more resistance to factual failures as opposed to ABS-Z where brittle delamination was noted due to low interlayer adhesion. Figure 5 illustrates CF-ABS malfunctions. CF-ABS-X retained its structural integrity with increased UTS, whereas CF-ABS-Z fractured prematurely supporting the anisotropy trends. Visual evidence of failure modes helps in interpreting the behavior of materials under tensile loading. Connected with numerical data, these results provide a deeper insight into fracture mechanisms and anisotropic materials behavior. Three samples for apiece material (ABS and subtype CF-ABS) were printed in the X, Y and Z direction respectively according to ASTM D638 standard. A total of 18 tensile test samples were obtained in this way (2 materials × 3 orientations × 3 replicates). Average values from these three replicates of Ultimate Tensile Strength (UTS), Yield Stress, Break Strength, Ductility and Young’s Modulus were calculated to establish statistical dependability. The SD for each group was also determined to demonstrate experimental variation.

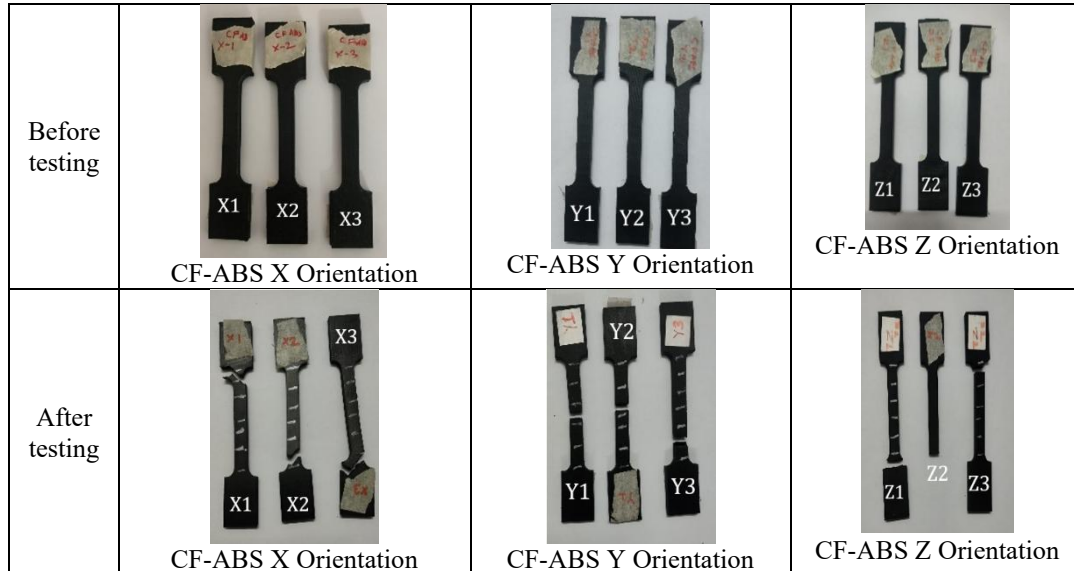


Figure 5: Tensile printed and tested X, Y and Z CF-ABS samples illustrating the influence of orientation. Source: Authors, (2026).

Advanced microstructural characterizations and full fatigue tests were not attempted in the present report to keep focus and convince of feasibility. These issues are discussed as potential research directions in the Future Research Directions section.

#### IV. RESULTS AND DISCUSSIONS

In this section, the experiment outcomes of tensile tests of FDM-printed ABS and CF-ABS samples at various build orientations are reported and discussed. The results are interpreted to determine the effect of material type and build direction on tensile strength, elastic modulus and elongation at break. Trends are sought and discussion is provided as to the observed mechanical behavior, related to FDM process sensitivity. Tensile test consequences for FDM-printed ABS and CF-ABS samples in X, Y, and Z build directions are given in Table 8.

The results indicate that there are prominent variations on mechanical properties depending on material composition and printing orientation. The ABS-Y specimens exhibited the superior UTS of 23.48 MPa and a Young’s modulus of 2077.26 MPa (stiffness), which contributes to improve the stiffness and load bearing in this direction. On the other end of the range, ABS-Z samples presented the lowest mechanical properties, with a UTS value as low as 4.93 MPa and even very diminished Young’s modulus (321.48 MPa), thus underlining the natural anisotropy in filament-based printed materials where an influence by interlayer adhesion was shown to be especially important.

The experimental conditions and outcomes listed in Table 8 are a result of an organized DOE approach, which samples were manufactured and tested according to controlled parameter settings, to establish the influence of material type and build orientation on mechanical behavior. The DOE method was beneficial for systematic evaluation by ensuring statistical dependability and revealing significant patterns of tensile properties. These findings provide crucial insight into the anisotropic behaviors of FDM-printed materials and underscore the need for promoting build orientation to achieve improved mechanical performance. The distinct features of CF-ABS, especially in the X and Y directions, suggest its value for such applications that require enhanced tensile strength and rigidity.

Table 8: Tensile test for ABS and CF-ABS samples in various building orientations.

Material-Orientation	Maximum Load (N)	UTS (MPa)	Ductility	Break Strength (MPa)	Yield Stress (MPa)	Young’s Modulus (E) (MPa)
ABS-X	635.56	15.86	3.01	10.93	13.75	452.74
ABS-Y	933.89	23.48	1.06	9.71	21.82	2077.26
ABS-Z	219.33	4.93	0.80	2.40	2.31	321.48
CF-ABS-X	1162.67	28.90	1.20	19.51	27.39	2296.65
CF-ABS-Y	826.00	20.40	0.67	20.14	18.45	2802.03
CF-ABS-Z	201.00	5.05	5.68	4.14	3.68	62.44

Source: Authors, (2026).

The specimens reproduced in the Y-orientation are found to have higher tensile properties than those printed in the X-orientation, as a result of better inter-layer bonding along loading direction. On the other hand, Z-oriented specimens can exhibit premature fracture due to poorer adhesion between layers (a common pattern in FDM process mechanics).

#### IV.1 ULTIMATE TENSILE STRENGTH

UTS of ABS and CF-ABS were evaluated for the X, Y, and Z orders. The results demonstrate significant material composition and print orientation dependences. Polymers ABS Material: Y-orientation (23.48 MPa), and X-orientation (15.86 MPa) had the highest UTS value, respectively. The lowest strength was achieved from the Z-orientation (4.93 MPa) due to poor interlayer bonding. 3.2 Comparison analyses of CF-ABS sample The UTS of the as-printed X-CF-ABS was found to have the highest value (28.90 MPa), and a significant improvement relative to ABS. However, Y-orientation had a slightly less UTS (20.40 MPa.) and still is considered the weakest in Z-orientation (5.05 MPa) similar to ABS. Y-orientation still provides the highest level of strength for ABS, likely due to better bonding between layers, while Z-orientation is weak in both cases because of delamination.

The comparatively reduced strength characteristics observed of Z-oriented specimens seem to be primarily resulted from the layer-by-layer printing technique that is typical for FDM, since in such case out-of-plane interlayer adhesion perpendicular to the loading direction is certain [4], [9]. However, poor interlayer adhesion is not the only cause. There are a few other things that contribute to this hole. First, the cooling rate gradient along the build height gives rise to thermal stresses that weaken the adhesion between successive layers; each layer deposited cools faster than its underlying one, leading to non-uniform solidification, different tract shrinkage and high residual stress on each layer where in turn will promote the generation of micro-voids and regions of concentrated stresses [21], [27], [30]. Furthermore, the repeated thermal cycling during deposition introduces internal stresses and partial debonding at the fiber-matrix interfaces [8], [14] which again detracts from interlaminar strength.

These effects – fiber asymmetry, rapid solidification, void formation and internal stress buildup – all contribute to decreasing the tensile strength and modulus in the Z-orientation more than just poor interlayer bond [9], [23], [27]. UTS for CF-ABS-X was the highest (28.9 MPa), which placed next ABS-Y (23.48 MPa). That is in line with the findings reported by [3] who reported approximately 21 MPa tensile strength of CF-ABS with 50% infill and hexagonal pattern. In same line, the present study can find [1] reported that CF-ABS with 80% infill had tensile strength of 36.9 MPa, which was a higher value compared to the present result and it was likely due to its higher infill density. In the end, while this experiment values are somewhat lower, the trends the present study seen seem to fit well with enhancements reported for CF incorporation and orientation optimization. A comparison of the UTS and ductility for ABS and CF-ABS coupons in different build directions (X-, Y- and Z-axis) is depicted in Figure 6. The bar chart illustrates the UTS (in MPa) for every material, and the line chart displays their corresponding ductility (elongation in %).

#### IV.2 ELONGATION OR DUCTILITY

The ductility provide information on how much the material can bend before it will break. Ductility Trends ABS: The maximum elongation was obtained in X-orientation (3.01%), followed by Y-direction (1.06%) and Z-direction (0.80%). CF-ABS: In the other trend, ductility ratio in Z direction (5.68%) was higher than that of X and Y directions (1.20%, 0.67%). It has been revealed that the failure modes were influenced by carbon fiber reinforcement, especially an improvement in interlayer adhesion in the Z-direction. Ductility and UTS are inversely related since greater orientations have lower elongations. UTS is improved while elongation is decreased by CF-ABS in X and Y directions. The Z-orientated CF-ABS exhibits a surprising increase in ductility which suggests fibre orientation influences in the weaker layers. Comparison of UTS and ductility between ABS-F and CF-ABS at different orientations are presented in Figure 6.

UTS and ductility for ABS and CF-ABS are scrambled with the printing orientations (X, Y, Z). UCT The tensile strength of CF-ABS material exceeds pure ABS in X-orientation (28.90MPa to 15.86MPa). For Y orientation, ABS has the maximum UTS (23.48 MPa) and CF-ABS has slightly lower value of 20.40 MPa. For materials in Z-orientation, the two exhibit the lowest UTS: 4.93 MPa for ABS and 5.05 MPa for CF-ABS. This is reasonable, as adhesion from layer-to-layer is weaker on this position. Ductility Evaluation: ABS-X (3.01%) and CF-ABS-X (1.20%) are found to have moderate ductility, with higher than that for pure ABS. The results demonstrate the Y-orientation has the lowest ductility (ABS: 1.06%, CF-ABS: 0.67%) together with higher UTS, suggesting a trade-off between strength and ductility.

Remarkably, the ductility of CF-ABS is considerably higher (5.68%) than that of ABS (0.80%) in Z direction, which might be attributed to enhanced interlayer adhesion achieved by CF enhancement. This is consistent with Figure 6, and it is confirmed that CF-ABS improves the tensile strength, particularly in X-orientation, but brings down ductility. On the other hand, with CF-ABS in Z orientation, ductility is significantly improved that may be good for some applications. As expected, tensile elongation at broken value of ABS samples were higher than CF-ABS. For example, the tensile ductility of ABS-Y samples was nearly two times higher than CF-ABS-Y. The limiting of ductility due to the addition of CF has been highlighted by [7], revealing that there was an increase in stiffness due to glass fiber restraint and strain capability decreased.

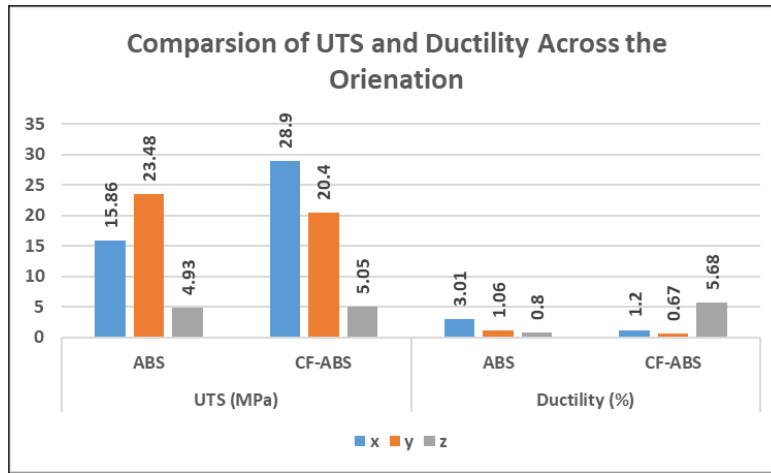


Figure 6: Bar chart comparing ultimate tensile strength (UTS) and ductility (%) of ABS and CF-ABS across X, Y, and Z orientations.

Source: Authors, (2026).

### IV.3 YOUNG'S MODULUS

The modulus of CF-ABS-Y (2802 MPa) exceeded ABS-Y (2077 MPa), demonstrating approximately 35% increase. This is reliable with what previous studies indicate by [3] and a 1470 MPa modulus was reported for Cf-ABS between [14], who reported an increase of 58% in flexural modulus for CF-ABS comparing with ABS. The increase in moduli found in this study may be explained by the denser infill (100%) employed and finer print settings, which decreased the porosity.

### IV.4 ORIENTATION DEPENDENCE

From the results, it is clear that Y-orientation printed specimens have better tensile strength because of enhances inter-layer connection in line with loading. In comparison, Z-oriented samples fail at an early stage due to weak layer bonding, which is in accordance with the FDM process being inherently anisotropic. For both materials, the Z-orientation specimens showed consistently lower performance and UTS decreased by more than 40% compared to those in X and Y orientations. By [4] and [9] have reported similar orientation-dependent anisotropy, with tensile strength reduction between 44 and 50% when comparing flat ( $0^\circ$ ) to upright ( $90^\circ$ ) orientations. Therefore, the present study like to highlight that poor adhesion between the layers is the principal limitation for Z-direction computer-controlled fabrication. Z-oriented samples collapse at low strains because of the poor interlayer bonding and residual thermal stress, which is characteristic to FDM process [11], [23]

The embedded carbon fibers act as the load-carriers, perfectly transferring stress from the polymer matrix to the stiffer fiber phase, resulting in upsurges in together tensile strength and elastic modulus [24], [26], [30]. In addition, the carbon fibers reduce the total thermal expansion coefficients and improve dimensional stability during printing due to denser layer interfaces and reduced warping [32], [35], [37]. This bonding at the fiber–matrix interface restricts polymer chains motion, which contributes to the increased stiffness as well as greater stress resistance under tensile loading [38], [42]. But these improvements come with certain concessions. Reduced chain mobility and stress localization at the fiber ends reduces ductility and strain to failure, contributing to a more brittle fracture behavior [44], [48]. Besides, introducing of carbon fibers a little bit more complex expelling process is encountered during extrusion; therefore, wear and tear of the nozzle are greater and need to deal with well-controlled print temperature for avoiding channel clogging and causing an uneven consumption.

Despite these limitations, the mechanical advantages of CF-ABS—particularly its increased strength, stiffness and interlayer adhesion—make it a compelling choice for structural or load-bearing applications where stiffness takes precedence over pliancy. Poor mechanical performance observed in Z-pullout samples is due not only to weak interlayer bonding but also to the thermo-mechanical response specifics of FDM process. During printing, the polymer filaments are deposited layer-wise in the direction of Z-axis leading to interfaces normal to the tensile load. This alignment concentrates stress between the layers, aiding in crack initiation and rapid delaminating under tension. Furthermore, the rate of cooling in the build direction is slower and not uniform as that along the X–Y plan, which leads to residual thermal stress and poor diffusion across layers. Reduced entanglement of the polymer chains, entrapped voids and nonuniform thermal gradients leads to less adhesion between layers then the X–Y plane, leading to lower tensile strength and stiffness in the Z-direction.

### IV.5 STRESS STRAIN CURVE

The mechanical properties of ABS and CF-ABS with different orientation were characterized by stress-strain curves. The Y-orientation curves of both ABS and CF-ABS exhibit the greatest stiffness, which is consistent with the highest Young's modulus. CF-ABS-X orientation has the largest stress response, indicating its high load-bearing capacity. Z-orientation curves remain flat, indicating a brittle fracture through poor interlayer adhesion. Figure 7 demonstrations the stress–strain curves of ABS and CF-ABS specimens at different orientations. The steepest slopes represent Y-orientation of both the materials, demonstrating maximum stiffness and Young's modulus. CF-ABS-X has the best tensile response behaviour between all the samples and it is associated with its good load bearing ability.

ABS-Z and CF-ABS-Z reveal poorest performance indicating very low stress values since poor interlayer adhesion limits the cohesion of the material layers. The conclusion is the reinforcing CF-ABS have significantly improved the stiffness and loading capacity of the composite materials, especially in X- and Y-direction as shown in Figure 7.

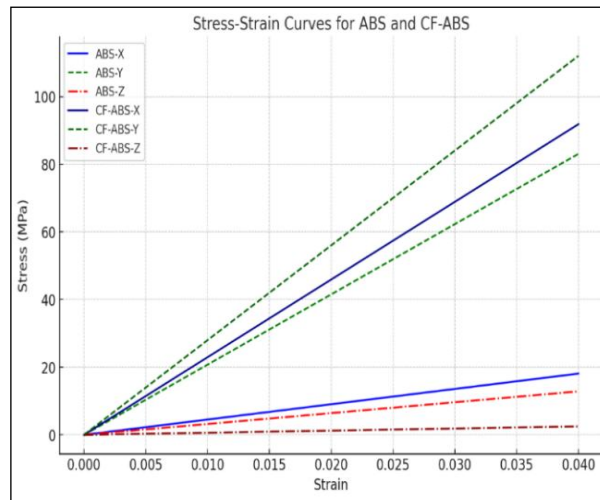


Figure 7: Stress-strain curves for ABS and CF-ABS. Source: Authors, (2026).

**IV.6 TENSILE STRENGTH RESULTS THROUGH LITERATURE COMPARISON**

In command to verify the tensile behavior of FDM-printed ABS and CF-ABS, the UTS values obtained were compared with the referred literature standards. In the following work, ABS also exhibited the superior UTS in ABS-Y (23.48 MPa) higher than that of ABS-X (15.86 MPa), and significantly higher than that of ABS-Z (4.93 MPa) due to remarkable weak inter-layer bonding. Also, CF-ABS had the highest UTS value in case of CF-ABS-X (28.90 MPa) and hence exhibits lowest UTS value for CF-ABS-Z (5.05 MPa) proving a significant axis-dependent anisotropy (Table 8). By [1] reported 36.9 MPa at 80% infill, showing higher cell density leads to higher strength. For CF-ABS, [3] were able to achieve ~21 MPa at 50% infill which approximately in-line with the current CF-ABS-Y (20.40 MPa). Therefore, the CF-ABS-X UTS (28.90 MPa) is suitable performance for CF-ABS.

In general, this comparison authenticates the validity of current results and emphasizes on the influence of material and build orientation under uniform loading situation. The trend X/Y > Z, is in agreement with previous research [9-11], where the failure of specimens oriented parallel to the Z-axis occurs prematurely as tensile loading is applied perpendicular to deposited layers and inter-layer fusion interfaces. [13], [14] observed the tensile degradation in vertical positions to be significant as a result of polymer diffusion being limited and therefore bonding weakened.

Table 9: Comparison of UTS Results with Published Literature.

Study	Material	Key Print Condition / Note	Reported UTS (MPa)	Comparison with Present Study
Present study	ABS	Y-orientation (best for ABS)	23.48	ABS-Y = 23.48 MPa (Reference value)
Present study	CF-ABS	X-orientation (best for CF-ABS)	28.90	CF-ABS-X = 28.90 MPa (Reference value)
Karupaiah and Narayanan [3]	CF-ABS	50% infill, hexagonal pattern	~21	Close to CF-ABS-Y = 20.40 MPa
Turaka et al. [1]	CF-ABS	80% infill	36.9	Higher than present due to higher infill
Syaefudin et al. [9]	ABS	Orientation-dependent ABS study	Orientation trend confirmed	Confirms X/Y > Z for ABS
Anubhav et al. [4]	ABS	Orientation anisotropy in FDM tensile	Orientation trend confirmed	Confirms Z weakest due to weak interlayer fusion

Source: Authors, (2026).

**IV.7 DISCUSSION ON MECHANICAL BEHAVIOUR OF CF-ABS**

The high tensile strength value of CF-ABS can be attributed to the good load transfer from the polymer matrix to the incorporated carbon fibers. The stiff fibers lower the overall ductility of the composite, as indicated by its low elongation-at break compared to unmodified ABS. Therefore, while CF-ABS has the same high level of stiffness and strength, it slightly sacrifices flexibility and processability. These effects must be balanced through parameters tuning to achieve both good mechanical properties and print quality. This is due to the fact that while carbon fibers increase stiffness and load carrying capability, they also result in decreased ductility and a more brittle fracture mode. Despite the enhanced mechanical properties, the processing of CF-ABS is problematic owing to nozzle abrasion of clogging and fiber clustering.

In comparison to the tensile response, macroscopic observations of fractured CF-ABS samples (Figure 5) offer some knowledge on failure as well. In the case of CF-ABS samples, a diminished necking and relatively sudden break was observed in comparison to neat ABS ones that is indicative of the higher stiffness brought by the CF-ABS. Samples made of CF-ABS oriented along the Z-axis exhibited an early interlayer delamination, demonstrating that layer-to-layer adhesion was a controlling factor for failure. These macroscopic observations help in rationalizing the tensile trends obtained experimentally and verify the anisotropic behavior of FDM printed CF-ABS parts.

**IV.8 MAIN EFFECT PLOTS**

In all orientations, CF-ABS reported significantly higher maximum load than pure ABS. The highest maximum load measured was obtained for CF-ABS in the X-orientation with 1162.67 N and the lowest maximum load of 201.00 N for CF-ABS in the Z-orientation. For both ABS (635.56 N) and CF-ABS (1162.67N), X-orientation occurred to be where the highest maximum loads were achieved, indicating good interlayer bonding when printed along this direction.-orientation also did comparatively well, -value of 933.89N for ABS and 826.00N for CF-ABS ) The Z-orientation gave the worst of both materials, probably due to poor interlayer adhesion (219.33 N and 201.00 N for ABS and CF-ABS). During tensile applications the structural weakness of CF-ABS is obvious since it has a higher load carrying capability than that reported for ABS, particularly in X-orientation.

The primary effect plot of S/N ratio is depicted in Figure 8 since the effects of build site and material type on the maximum load (N). Higher UTS was detected in CF-ABS samples related to ABS samples. CF-ABS-X had the greatest UTS (28.90 MPa) but ABS-Z did not exceed 4.93 MPa. X-orientation: ABS (15.86 MPa) and CF-ABS (28.90 MPa) exhibit the maximum UTS. In the Y-orientation the values are slightly by CF-ABS (20.40 MPa) and better in ABS (23.48 MPa). Z-orientation has the least UTS (4.93 MPa in ABS, 5.05 MPa in CF-ABS), because their inter-layer bonding is low. The failure in the Z-orientation results from the delamination of layers. For the two materials, the X and Y directions have highest strength. The interaction plot for S/N ratios is depicted in Figure 9, the consequence of build direction and material on UTS.

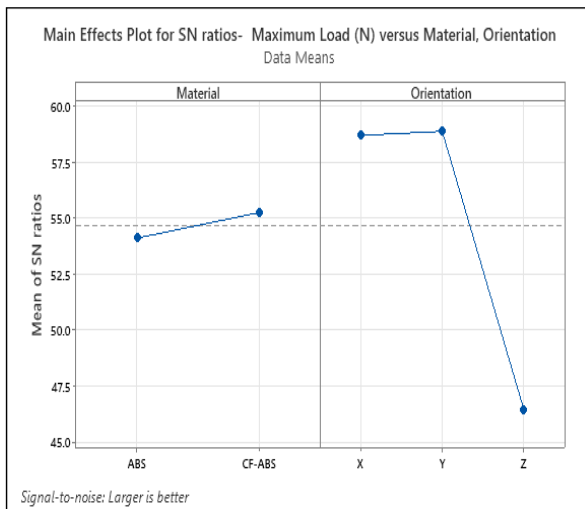


Figure 8: Main effect plot for SN ratios Maximum Load (N) versus Material, Orientation. Source: Authors, (2026).

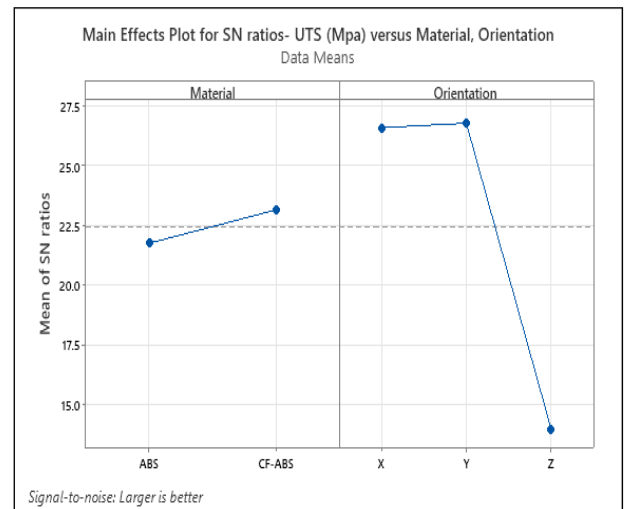


Figure 9: Main effect plot for SN ratios UTS (MPa) versus Material, Orientation. Source: Authors, (2026).

The tensile strength of CF-ABS was improved. CF-ABS-Y showed the highest break strength (20.14 MPa), which may be associated with orientation-dependent load transfer and failure behaviour. CF-ABS-X came next with 19.51 MPa, revealing excellent strength at this direction. The maximum tensile strength was 20.14 MPa (in CF-ABS-Y) and the lowest was 2.40 MPa (in ABS-Z). Polymers in ABS-X and ABS-Y are characterized with lower tensile strengths at break (i.e., 10.93 MPa, 9.71 MPa, respectively). The introduction of a carbon micro pipe structure strongly improves sandwich properties, in particular strength and rigidity. Early failures were the ABS-Z and CF-ABS-Z with very low brake strength (2.40 MPa, 4.14 MPa). Z-orientation is not suitable for tension application because of its brittle failure. The primary effects plot for S/N ratios is presented in Figure 10, and it investigates the stimulus of build orientation and material type on break strength.

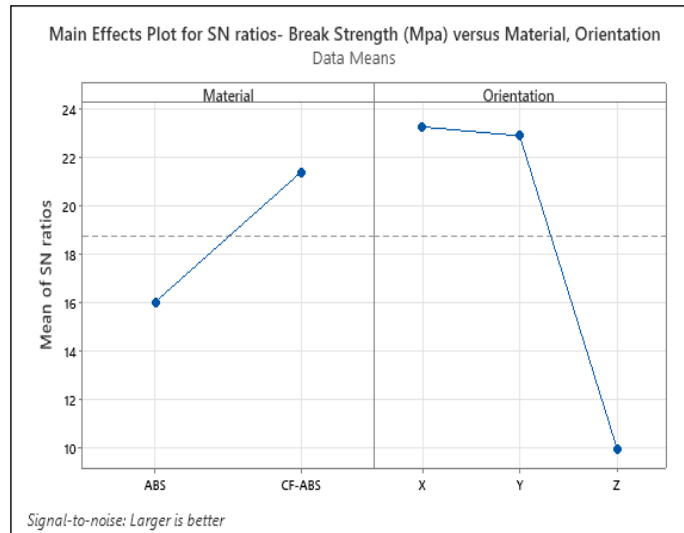


Figure 10: Main effect plot for SN ratios UTS (MPa) versus Material, Orientation. Source: Authors, (2026).

CF-ABS exhibited stronger performance than ABS; CF-ABS-X had the highest yield stress of 27.39 MPa, while ABS-Z has the bottom (2.31 MPa). X-Orientation: The yield stress of CF-ABS (27.39 MPa) and ABS (13.75 MPa) were the highest. Y-orientation: ABS performed better (21.82 MPa) and CF-ABS had an acceptable value (18.45 MPa). Z-orientation: This is the least strong orientation with 2.31 MPa (ABS) and 3.68 MPa (CF-ABS). In particular, the CF-ABS substantially enhances yield stressing, particularly along X-orientation. Perhaps due to stress transfer, ABS-Y exhibits a higher yield strength than CF-ABS-Y. Due to its bad adhesion, the Z-oriented cut has the least good yield properties. The main effect plot for signal-to-noise (S/N) ratio is presented in Figure 11 which demonstrates the things of build orientation and material type on yield stress (MPa).

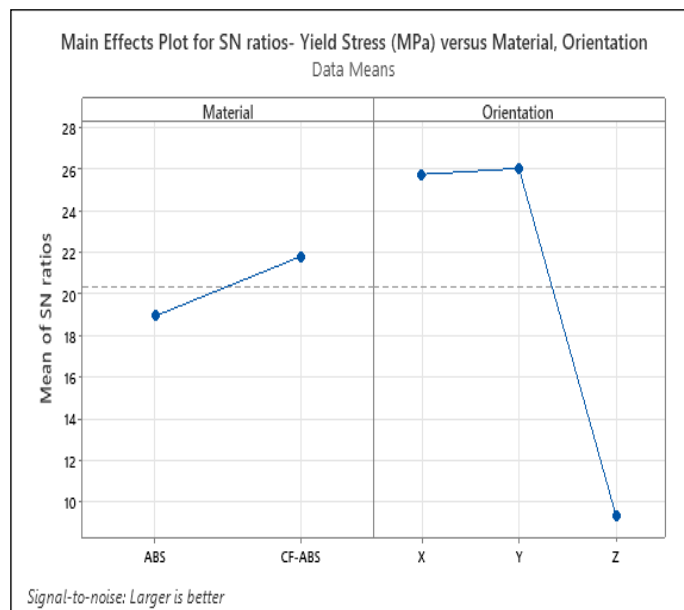


Figure 11: Main effect plot for SN ratios – Yield Stress (MPa) versus Material, Orientation. Source: Authors, (2026).

Figure 11: Yield Stress (MPa) vs Material main effect plot for SN ratios Orienta In all orientations CF-ABS had higher Young’s modulus which means its stiffness is high. The maximum reported was 2802.03 MPa by CF-ABS-Y and the minimum of 62.44 MPa by CF-ABS-Z. Y-direction: ABS was the strongest (2077.26 MPa), and CF-ABS had the highest stiffness (2802.03 MPa). X-orientation: ABS (452.74 MPa) is worse than CF-ABS (2296.65 MPa). Z: Low stiffness (62.44 MPa for CF-ABS, 321.48 MPa for ABS). CF-ABS significantly increases Young’s modulus, so it is great for structural parts. Z-orientation is weak due to low rigidness and is not good for load bearing purposes. Z is the weakest, followed by X and then Y. The main effect plot for S/N ratios is given in Figure 12 which considers the effects of build orientation and material type on E in (MPa).

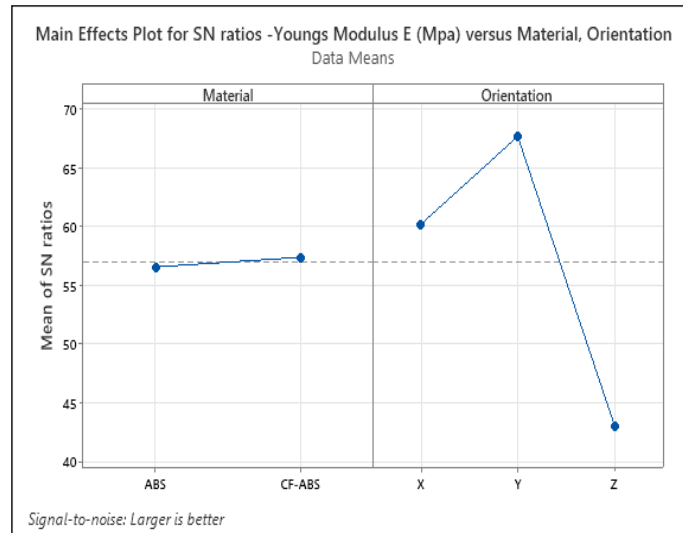


Figure 12: Main effect plot for SN ratios - Young's Modulus E (MPa) versus Material, Orientation. Source: Authors, (2026).

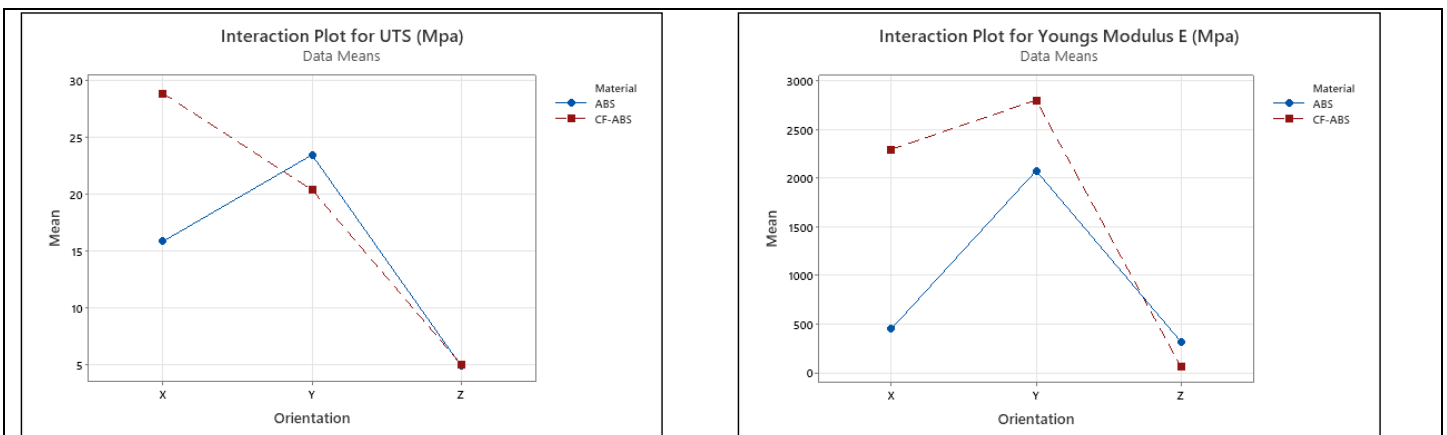
In the case of ABS, CF-ABS shows a huge improvement in all mechanical properties. **Orientation Variability:** shows maximum overall performance towards Young's modulus, break strength and UTS. Next, the present study placed X-orientation, which has moderate stiffness but is strong. Since the Z orientation exhibits weak interlayer bonding, it is not recommended for tensile load-bearing applications. **Failure Modes:** In the Z-orientation, weak interlayer bonding or delamination led to failure. Y and X orientations present better load-bearing capacity and crack-resistance. **Design Implication:** For strong parts, print CF-ABS in X or Y directions. The inclination and material type have large effects on mechanical properties are also supported by S/N analysis.

#### IV.9. INTERACTION PLOT

The most significant effects of the orientation and material (ABS versus CF-ABS) are shown in Figure 13 for selected mechanical parameters. **UTS:** the UTS of CF-ABS is significantly higher in X (28.90 MPa) than that of ABS (15.86MPa). Although CF-ABS-X showed the highest UTS, the Y-orientation exhibited competitive tensile performance; this variation may be attributed to fibre alignment effects and interlayer bonding characteristics. Similarly, the Z-orientation remains to be the weakest for both materials.

- **Young's modulus:** CF-ABS-Y has excellent load bearing capacity with the highest stiffness (2802 MPa). Y-orientation is also the highest performing orientation, with a strong ABS-Y (2077 MPa). Low stiffness is observed in Z-direction, particularly for CF-ABS (only 62 MPa).
- **Yield Stress:** For CF-ABS-X and ABS-Y, the same ranking was observed as for UTS. The Z-orientation is the worst for both materials.
- **Break Strength:** The maximum break strength (~20.14 MPa) is shown in Y-orientation for CF-ABS. Orientation in Z remains the weakest, while orientation along X is also strong.

These graphs provide some evidence for the idea that Y-orientation is best for ABS and X-orientation is best for CF-ABS due to better fiber alignment.



A. Interaction plots for UTS, Young's Modulus, and Yield Stress & Break strength with orientation

B Interaction plots for Young's Modulus with orientation

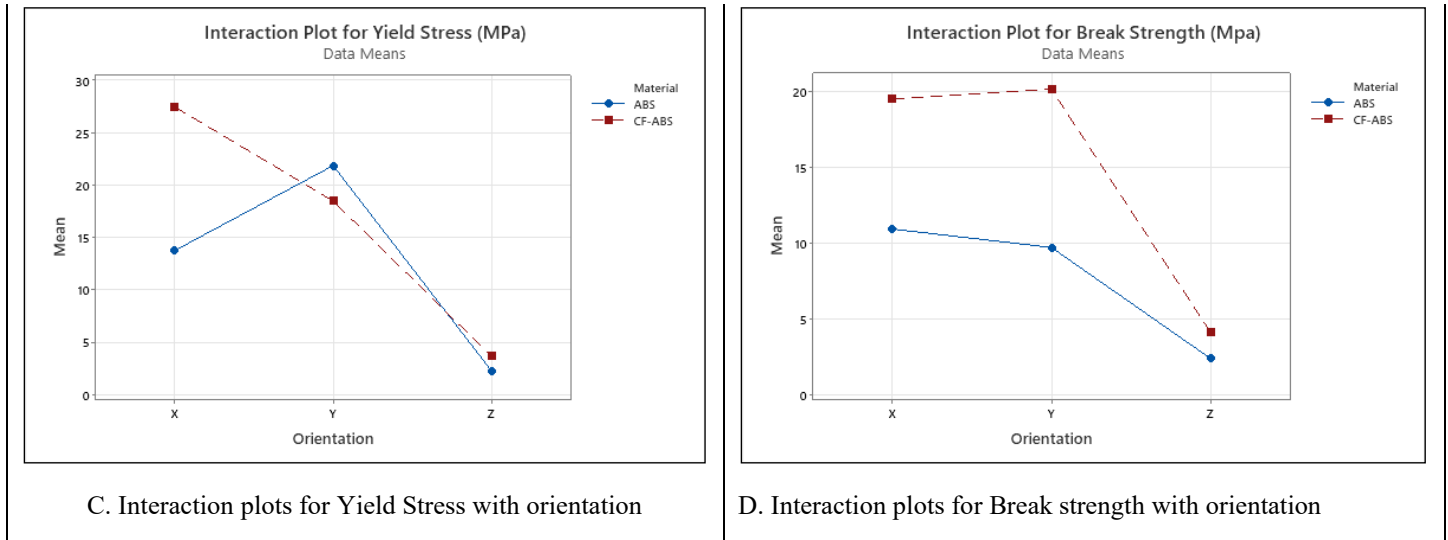


Figure 13: Interaction plots for UTS, Young's Modulus, and Yield Stress & Break strength with orientation.  
Source: Authors, (2026).

#### IV.10 FAILURE MODE INTERPRETATION

The failure behaviour of FDM-printed ABS and CF-ABS tensile samples were markedly affected by the build orientation, indicating that the inherent anisotropy involved layer-by-layer fabrication. Discrepant fracture behavior in the X-, Y- and Z-oriented samples may be due to different interlayer bonding strength and load transfer efficiency [48], [49]. X and Y oriented parts in-plane tensile failure, where the load applied was parallel to filament deposition. A higher tensile strength and stiffness of these orientations were presented by an enhanced stress distribution and the more intense interlayer fusion, where the Y orientation displayed also the most sustained fracture process [50–53].

Z-oriented specimens suffered from early interlayer delamination due to the tensile action being perpendicular to the layer that are stacked. This led to a brittle fracture with low-ductility nature, which was dominated by poor adhesion of the interlayer rather than strength of filaments [54–57]. The CF-ABS samples presented a higher stiffness and a lower ductility with respect to the neat ABS, suggesting an evolution toward more brittle failure. The reinforcement of short carbon fibers was better in X- and Y-directions with the failure continued to be controlled by interfacial strength and fibre continuity in the Z direction across layers [58], [63-65]. In general, the data demonstrate that the role of build orientation in failure behavior is more pronounced than that of material type and underscores the significance of orientation-aware design criteria when employing CF-ABS filaments for load-carrying FDM applications [59–62].

The current work aimed to examine influence of build orientation and physical type on quasi-static tensile act FDM-printed ABS and CF-ABS samples at constant processing parameters. Other key variables like raster angle, layer thickness, and extrusion temperature or infill pattern were deliberately fixed to isolate orientation effects which constrains the direct transferability of the findings to other parameter combinations [46], [54]. Moreover, the procedure was limited to monotonically loaded tension and a detailed analysis of microstructure information including fracture surfaces was not within the scope of this study [55], [59]. Further work is needed for the more detailed evaluation of the performance of CF-ABS for load-bearing applications including microstructure assessment, fatigue properties and multi-parameter optimization [60–62].

#### V. CONCLUSIONS

Orientation dependent tensile properties of ABS and CF-ABS composite prepared by FDM were examined in the existing work. It can be observed from the consequences that material and build orientation significantly influenced the mechanical performance:

- The highest rigidity (2077.26 MPa) and the UTS value (23.48 MPa) exhibited the orientation ABS-Y.
- CF-ABS-X orientation showed the reinforcing effect of carbon fibers with their highest UTS (28.90 MPa).
- Because of poor interlayer bonding, the Z-directional samples invariably demonstrated low strength and modulus.
- ABS is also more ductile than CF-ABS, which makes it that reducing strength to increase ductility.

In general, CF-ABS is more suitable for structural and loadbearing applications because carbon fibers dramatically improved tensile strength and stiffness with particular dominance in X and Y directions. Yet, its application in systems that require large flexibility might be restricted due to the decreased stretchability. Use CF-ABS (20%) in the X or Y position for parts requiring high Structural rigidity: brackets, holders, holsters etc. For applications that need flexibility or impact absorption, plain old ABS may still be better. The following conclusions were drawn from these experimental studies of FDM-printed orientation-dependent tensile behavior of ABS and CF-ABS.

- Anisotropy is regulated by direction: Z-orientation consistently produced the lowest strength due to weak interlayer bonding while Y-orientation in ABS and X-orientation in CF-ABS showed the highest tensile mechanical performance.
- The modulus of CF-ABS samples was 35% higher and the UTS approximately 25% greater than that of neat ABS, which confirmed that carbon fibers enhanced stiffness.

- Trade-off of strength and ductility: CF-ABS improved strength while reducing ductility, meantime neat ABS is better in applications that requires flexible or impact resistant.
- Trends supported by DOE-based analysis: Taguchi main-effect and S/N plots provided evidence of orientation and material being the two most influential parameters for tensile behavior.
- Experimental values correlate with previous research: The credibility of the data is enhanced as UTS and modulus show good agreement with other work on CF-ABS.
- Applications: Neat ABS can still be used when no structural bending is desired in the part, but it doesn't make sense for load bearing parts. CF-ABS printed in the X or Y orientations is more suitable for structurally relevant components.

A mannered analysis on tensile properties of FDM-printed ABS and CF-ABS parts in different building orientations was conducted in this study. The results demonstrate how material type and build orientation collectively influence UTS, yield stress, ductility and stiffness including material orientation and composition influence the mechanical performance, most notably yield stress, ductility, Young's modulus and ultimate tensile strength (UTS). The results demonstrate that the mechanical response of FDM-printed specimens is sturdily affected by construction orientation. Among all tested configurations, Y-oriented CF-ABS specimens had the highest mechanical strength (Young's modulus of 2802.03 MPa and UTS of 20.40 MPa). In contrast, poor interlayer adhesion led to very bad mechanical properties for both the Z-oriented samples of all material compositions; CF-ABS-Z being the worst (UTS = 5.05 MPa, Young's modulus = 62.44 MPa).

The ductility of ABS and CF-ABS materials exhibited a different trend; pure ABS presented higher elongation in the X and Z directions (3.01% and 0.80%, respectively), while the high stiffness of CF-ABS caused a reduction in its penetration capacity in all directions. Decision about stiffness and flexibility trade-off When the design of functional FDM parts with high tensile strength, there is possible to take into stiffening and correlatively flexible. With tensile strengths (UTS) 23.48 MPa and 20.40 MPa for ABS and CF-ABS, respectively, the Y-direction yielded the top tensile strength and stiffness in all cases. The X-oriented CF-ABS specimens possess greatly higher UTS (28.90 MPa) and elastic modulus (2296.65 MPa) than the all-other configurations, representing enhanced load-carrying capability by CF-ABS. The Z-orientation showed on the contrary to have the worst mechanical behavior which resulted in much lower values of UTS (4.93 MPa for ABS and 5.05 MPa for CF-ABS) and no resistance under tensile stress, thus highlighting also in this case (80%) its anisotropy of FDM printed materials.

Moreover, the results demonstrate ductility has been decreased with advance in tensile strength and modulus due to the incorporation of CF-ABS, predominantly in X- and Y-directions. CF-ABS can be used for applications requiring higher structural strength and mechanical durability in components made by additive because of its greater stiffness that is indicative of better load transfer effectiveness. The work expands the material design space of FDM thermoplastic composites and additive manufacturing in generality. The measurement technique provides quantitative verification of the effect of layers orientation and CF-ABS mechanical properties. In terms of bearing load, the CF-ABS was found to be a much better candidate than neat ABS for load-carrying applications, particularly in the Y-axis where tensile stress is distributed throughout coextruded fiber channel. The findings are also consistent with previous studies showing that layer bonding in the Z-direction is essentially poor requiring intentional modifications for applications demanding isotropic properties.

Moreover, the DOE-based method supplies a systematic approach to optimizing FDM parameters, thus enabling engineers and researchers to predict mechanical responses given material composition and printing orientation. This work sets the stage for further optimization investigation, particularly in hybrid and multi-material FDM printing. Although this work is a significant contribution, further studies are necessary to improve the mechanical belongings of FDM-printed composites. Future work should investigate: Advanced Infill Geometries: The influence of complex lattice structure and infill % on mechanical behavior. Failure analysis under cyclic loading conditions for long-term mechanical stability, is called fatigue and fracture analysis. Thermal and Environmental effects: Evaluate in performance at various humidity levels and temperature ranges, whether it's viable. FEA: Stress spread to predict modeling for design better solution. Multi-Material Printing Exploring dual-nozzle printing for structures with a functionally graded structure and gradient material properties.

This paper has demonstrated the influence of material arrangement and orientation on tensile behaviour for FDM parts. Although from the Z-structure perspective it still remains a drawback, CF-ABS exhibits significantly greater strength characteristics, especially at the Y axis. The insights from this work provide useful guidelines for developing stronger and more reliable FDM-printed polymer composites. The potential FDM has in high-performance is likely to be augmented as new hybrid materials, better deposition control and advanced computer modeling are developed. In general, mechanically motivated process design decisions for build orientation and material selection of FDM manufactured polymer and composite parts for load-bearing applications are presented here. Results of this work may be used to optimize mechanical performance while considering the inherent anisotropy of FDM process by designers and engineers.

## VI. STUDY LIMITATION

The tensile behavior of FDM-built ABS and CF-ABS specimens was studied in the present work, mainly focusing on the build orientation with fixed processing conditions. In order to attribute mechanical variability solely to orientation, parameters including raster pattern, layer height and thickness, infill percentage and extrusion temperature were deliberate kept constant which inherently limits the generalizability of the results into other parameter sets. Also, the testing program was limited to monotonic tensile loading and performance and behavior under cyclic fatigue, impact loading, time-dependent deformation, or environmental exposure were not considered. Furthermore, the microstructural and fracture-surface analyses were beyond the scope of this work such that a more detailed interpretation about fibre-matrix bond, internal void shape and interlayer damage mechanisms for (vertical-printed) specimens was narrowed down.

## VII. FUTURE RESEARCH DIRECTIONS

In the current research, parameter-based optimization studies of FDM printed ABS and CF-ABS parts are pilot attempt. As both X and Y build orientations consistently outperformed in terms of tensile behavior, the study will be narrowed down to ABS-X, ABS-Y, CF-ABS-X and CF-ABS-Y only for future designs [3], [9]. A Taguchi-based DOE of ~25 specimens will be used, by changing speed, layer thickness and infill density to establish optimum tensile properties [23], [30]. Tensile experimental results will be cross-validated with FEA under the same loading conditions to check numerical-experimental consistency [34], [44]. Moreover, hybrid ABS–CF-ABS specimens with different CF-ABS layer thicknesses will be fabricated and investigated using experimental tests FEA and analytical equations for load transfer efficiency and stiffness improvement [13], [24].

The present work is restricted to the quasi-static tensile behaviour of FDM printed ABS and CF-ABS test pieces for given printing conditions. Further microstructural analysis at a higher-level such as SEM fractography and calibrated X-ray attenuation from micro-CT based defect/void quantification was omitted, so the effect of fibre dispersion, porosity and interlayer defects with tensile failure could not be explicitly linked in a quantitative manner to the mechanical performance observed. Furthermore, long-term durability behaviour such as those under fatigue, creep and environmental ageing was not studied in the present work. In future work, will be directed towards a more advanced microstructure–property correlation and development of validated predictive tools through FEA which can possibly be complemented with ML techniques in order to improve reliability prediction of orientation-sensitive CF-ABS composite parts.

## VIII. AUTHOR'S CONTRIBUTION

**Conceptualization:** Kaustubh Pravin Joshi, M. K. Chopra.

**Methodology:** Kaustubh Pravin Joshi.

**Investigation:** Kaustubh Pravin Joshi.

**Discussion of results:** Kaustubh Pravin Joshi, M. K. Chopra.

**Writing – Original Draft:** Kaustubh Pravin Joshi

**Writing – Review and Editing:** Kaustubh Pravin Joshi, M. K. Chopra.

**Resources:** Kaustubh Pravin Joshi, M. K. Chopra.

**Supervision:** M. K. Chopra.

**Approval of the final text:** Kaustubh Pravin Joshi, M. K. Chopra.

## IX. ACKNOWLEDGMENTS

We thank the higher authorities of Sarvepalli Radhakrishnan University, Bhopal for their constant provision and reassurance.

## X. REFERENCES

- [1] S. Turaka, V. Jagannati, B. Pappula, and S. Makgato, "Impact of infill density on morphology and mechanical properties of 3D printed ABS/CF-ABS composites using design of experiments," *Heliyon*, vol. 10, pp. 1–25, Art. no. e29920, 2024, doi: 10.1016/j.heliyon.2024.e29920.
- [2] A. S. de León, A. Domínguez-Calvo, and S. I. Molina, "Materials with enhanced adhesive properties based on acrylonitrile-butadiene-styrene (ABS)/thermoplastic polyurethane (TPU) blends for fused filament fabrication (FFF)," *Materials & Design*, vol. 182, pp. 1–11, Art. no. 108044, 2019, doi: 10.1016/j.matdes.2019.108044.
- [3] V. Karupaiyah and V. Narayanan, "Quasi-static and dynamic mechanical analysis of 3D printed ABS and carbon fiber reinforced ABS composites," *Material Plastic*, vol. 59, no. 3, pp. 152–179, 2022, doi: 10.37358/Mat.Plast.1964.
- [4] Anubhav, R. Kumar, S. K. Nandi, and A. Agrawal, "Influence of build orientation on tensile and flexural strength of FDM fabricated ABS component," in *Advances in Additive Manufacturing and Metal Joining*, N. Ramesh Babu et al., Eds. Singapore: Springer, 2023, pp. 177–187, doi: 10.1007/978-981-19-7612-4\_15.
- [5] H. H. B. Hamzah, O. Keatch, D. Covill, and B. A. Patel, "The effects of printing orientation on the electrochemical behaviour of 3D printed acrylonitrile butadiene styrene (ABS)/carbon black electrodes," *Scientific Reports*, vol. 8, pp. 1–8, Art. no. 9135, 2018, doi: 10.1038/s41598-018-27188-5.
- [6] A. Q. Shurjeel, N. Pothula, and E. Punna, "Experimental investigation of strength properties of 3D printed ABS composites," *E3S Web of Conferences*, vol. 309, Art. no. 01148, 2021, doi: 10.1051/e3sconf/202130901148.
- [7] A. Dhandapani, S. Krishnasamy, N. Rajini, S. Siengchin, T. S. M. Kumar, M. Chandrasekar, K. Yorseng, "Thermal and tensile properties of 3D printed ABS-glass fibre, ABS-glass fibre-carbon fibre hybrid composites made by novel hybrid manufacturing technique," *Journal of Thermoplastic Composite Materials*, pp. 1–20, 2023, doi: 10.1177/08927057231170805.
- [8] O. Adeniran, W. Cong, and K. Oluwabunmi, "Thermoplastic matrix material influences on the mechanical performance of additively manufactured carbon-fiber-reinforced plastic composites," *Journal of Composite Materials*, pp. 1–15, 2022, doi: 10.1177/00219983221077345.
- [9] E. A. Syaefudin, A. Kholil, M. Hakim, D. A. Wulandari, Riyadi, and E. Murtinugraha, "The effect of orientation on tensile strength 3D printing with ABS and PLA materials," *Journal of Physics: Conference Series*, vol. 2596, Art. no. 012002, 2023, doi: 10.1088/1742-6596/2596/1/012002.
- [10] S. Alam, M. T. Hassan, J. Merrell, J. Lee, "Comparative analysis of water-induced response in 3D-printed SCF/ABS composites under controlled diffusion," in *SAMPE Conference Proceedings*, Long Beach, CA, USA, May 20–23, 2024.
- [11] J. Li and Y. F. Zhang, "The tensile properties of short carbon fiber reinforced ABS and ABS/PA6 composites," *Journal of Reinforced Plastics and Composites*, vol. 29, no. 11, pp. 1727–1737, 2010, doi: 10.1177/0731684409337551.
- [12] C. Rajesh, N. V. N. Kumar, and G. Gowthami, "Evaluation of wear behaviour of PLA and ABS parts fabricated by FDM technique with distinct orientations," *International Journal of Recent Technology and Engineering (IJRTE)*, vol. 7, no. 5S3, 2019.
- [13] J. Yan, E. Demirci, and A. Gleadall, "Single-filament-wide tensile-testing specimens reveal material-independent fibre-induced anisotropy for fibre-reinforced material extrusion additive manufacturing," *Loughborough University*, 2023. [Online]. Available: <https://hdl.handle.net/2134/23095364.v1>

- [14] K. Wang, S. Li, Y. Rao, Y. Wu, Y. Peng, S. Yao, H. Zhang, and S. Ahzi, "Flexure behaviors of ABS-based composites containing carbon and Kevlar fibers by material extrusion 3D printing," *Polymers*, vol. 11, Art. no. 1878, 2019, doi: 10.3390/polym11111878.
- [15] M. Moradi, Z. M. Beiranvand, N. Salimi, S. Meiabadi, and J. Lawrence, "Experimental investigation on the 3D printing of nylon reinforced by carbon fiber through fused filament fabrication process: Effects of extruder temperature and printing speed," *International Journal of Polymer Science*, Art. no. 1234797, 2024, doi: 10.1155/2024/1234797.
- [16] G.-W. Lee, T.-H. Kim, J.-H. Yun, N.-J. Kim, K.-H. Ahn, M.-S. Kang, "Strength of Onyx-based composite 3D printing materials according to fiber reinforcement," *Frontiers in Materials*, vol. 10, Art. no. 1183816, 2023, doi: 10.3389/fmats.2023.1183816.
- [17] A. Dhandapani, S. Krishnasamy, R. Nagarajan, A. D. A. Selvaraj, S. M. K. Thiagamani, C. Muthukumar, F. Mohammad, H. A. Al-Lohedan, S. O. Ismail, "Investigation of wear behavior in self-lubricating ABS polymer composites reinforced with glass fiber/ABS and glass fiber/carbon fiber/ABS hybrid," *Lubricants*, vol. 11, Art. no. 131, 2023, doi: 10.3390/lubricants11030131.
- [18] S. W. Ahmed, G. Hussain, K. Altaf, S. Ali, M. Alkahtani, M. H. Abidi, A. Alzabidi, "On the effects of process parameters and optimization of interlaminar bond strength in 3D printed ABS/CF-PLA composite," *Polymers*, vol. 12, Art. no. 2155, 2020, doi: 10.3390/polym12092155.
- [19] S. H. R. Sanei and D. Popescu, "3D-printed carbon fiber reinforced polymer composites: A systematic review," *Journal of Composites Science*, vol. 4, Art. no. 98, 2020, doi: 10.3389/jcs.2020.00098.
- [20] A. Grant, B. Regez, S. Kocak, J. D. Huber, and A. Mooers, "Anisotropic properties of 3-D printed poly lactic acid (PLA) and acrylonitrile butadiene styrene (ABS) plastics," *Results in Materials*, vol. 12, Art. no. 100227, 2021, doi: 10.1016/j.rinma.2021.100227.
- [21] J. Kluczyński et al., "Fatigue and fracture of additively manufactured polyethylene terephthalate glycol and acrylonitrile butadiene styrene polymers," *International Journal of Fatigue*, vol. 165, Art. no. 107212, 2022, doi: 10.1016/j.ijfatigue.2022.107212.
- [22] M. T. Birosz, D. Ledenyák, and M. Andró, "Effect of FDM infill patterns on mechanical properties," *Polymer Testing*, vol. 113, Art. no. 107654, 2022, doi: 10.1016/j.polymertesting.2022.107654.
- [23] S. Cicero et al., "Structural integrity assessment of additively manufactured ABS, PLA and graphene reinforced PLA notched specimens combining Failure Assessment Diagrams and the Theory of Critical Distances," *Theoretical and Applied Fracture Mechanics*, vol. 121, Art. no. 103535, 2022, doi: 10.1016/j.tafmec.2022.103535.
- [24] S. S. G. Iyer and O. Keles, "Effect of raster angle on mechanical properties of 3D printed short carbon fiber reinforced acrylonitrile butadiene styrene," *Composites Communications*, vol. 32, Art. no. 101163, 2022, doi: 10.1016/j.coco.2022.101163.
- [25] F. He, Y. L. A. Alshammari, and M. Khan, "The effect of printing parameters on crack growth rate of FDM ABS cantilever beam under thermo-mechanical loads," *Procedia Structural Integrity*, vol. 34, pp. 59–64, 2021, doi: 10.1016/j.prostr.2021.12.009.
- [26] S. Garzon-Hernandez, D. Garcia-Gonzalez, A. Jérusalem, and A. Arias, "Design of FDM 3D printed polymers: An experimental-modelling methodology for the prediction of mechanical properties," *Materials & Design*, vol. 188, Art. no. 108414, 2020, doi: 10.1016/j.matdes.2019.108414.
- [27] N. Yu, X. Sun, Z. Wang, D. Zhang, J. Li, "Effects of auxiliary heat on warpage and mechanical properties in carbon fiber/ABS composite manufactured by fused deposition modeling," *Materials & Design*, vol. 195, Art. no. 108978, 2020, doi: 10.1016/j.matdes.2020.108978.
- [28] A. Forés-Garriga, G. Gómez-Gras, and M. A. Pérez, "Mechanical performance of additively manufactured lightweight cellular solids: Influence of cell pattern and relative density on the printing time and compression behavior," *Materials & Design*, vol. 215, Art. no. 110474, 2022, doi: 10.1016/j.matdes.2022.110474.
- [29] K. M. Agarwal et al., "Analyzing the impact of print parameters on dimensional variation of ABS specimens printed using fused deposition modelling (FDM)," *Sensors International*, vol. 3, Art. no. 100149, 2022, doi: 10.1016/j.sintl.2021.100149.
- [30] P. Wang et al., "Effects of FDM-3D printing parameters on mechanical properties and microstructure of CF/PEEK and GF/PEEK," *Chinese Journal of Aeronautics*, vol. 34, no. 9, pp. 236–246, 2021, doi: 10.1016/j.cja.2020.05.040.
- [31] M. San Andrés et al., "Use of 3D printing PLA and ABS materials for fine art: Analysis of composition and long-term behaviour of raw filament and printed parts," *Journal of Cultural Heritage*, vol. 59, pp. 181–189, 2023, doi: 10.1016/j.culher.2022.12.005.
- [32] P. M. Angelopoulos et al., "Manufacturing of ABS/expanded perlite filament for 3D printing of lightweight components through fused deposition modeling," *Materials Today: Proceedings*, vol. 54, pp. 14–21, 2022, doi: 10.1016/j.matpr.2021.06.351.
- [33] W. Föster et al., "Mechanical performance of hexagonal close-packed hollow sphere infill structures with shared walls under compression load," *Additive Manufacturing*, vol. 59, Art. no. 103135, 2022, doi: 10.1016/j.addma.2022.103135.
- [34] K. A. Al-Ghamdi, "Sustainable FDM additive manufacturing of ABS components with emphasis on energy minimized and time efficient lightweight construction," *International Journal of Lightweight Materials and Manufacture*, vol. 2, pp. 338–345, 2019, doi: 10.1016/j.ijlmm.2019.05.004.
- [35] C. Abeykoon, P. Sri-Amphorn, and A. Fernando, "Optimization of fused deposition modeling parameters for improved PLA and ABS 3D printed structures," *International Journal of Lightweight Materials and Manufacture*, vol. 3, pp. 284–297, 2020, doi: 10.1016/j.ijlmm.2020.03.003.
- [36] M. H. Ali et al., "Development of a large-scale multi-extrusion FDM printer, and its challenges," *International Journal of Lightweight Materials and Manufacture*, pp. 198–213, 2023, doi: 10.1016/j.ijlmm.2022.10.001.
- [37] C. Aumnate, A. Pongwisuthiruchte, P. Pattananuwat, and P. Potiyaraj, "Fabrication of ABS/graphene oxide composite filament for fused filament fabrication (FFF) 3D printing," *Advances in Materials Science and Engineering*, pp. 1–9, 2018, doi: 10.1155/2018/2830437.
- [38] S.-H. Ahn, M. Montero, D. Odell, S. Roundy, and P. K. Wright, "Anisotropic material properties of fused deposition modeling ABS," *Rapid Prototyping Journal*, pp. 248–257, 2002, doi: 10.1108/13552540210441166.
- [39] A. K. Cress et al., "Effect of recycling on the mechanical behavior and structure of additively manufactured acrylonitrile butadiene styrene (ABS)," *Journal of Cleaner Production*, Art. no. 123689, 2021, doi: 10.1016/j.jclepro.2020.123689.
- [40] M. Mucha et al., "Effect of infill style and density on selected mechanical properties of the carbon fibre reinforced ABS MFD filament," in *34th Congress of the International Council of the Aeronautical Sciences*, 2024, pp. 1–10.

- [41] T. Appalsamy et al., “Tensile test analysis of 3D printed specimens with varying print orientation and infill density,” *Journal of Composites Science*, vol. 8, Art. no. 121, 2024, doi: 10.3390/jcs8040121.
- [42] N. Sayah and D. E. Smith, “Correlation of microstructural features within short carbon fiber/ABS manufactured via large-area additive-manufacturing beads,” *Journal of Composites Science*, vol. 8, Art. no. 246, 2024, doi: 10.3390/jcs8070246.
- [43] S. M. Nayak, P. B. Shetty, and J. S. Reddy, “Failure analysis of additively manufactured fibre reinforced acrylonitrile butadiene styrene (ABS) material by experimental and numerical method,” *Journal of Emerging Technologies and Innovative Research (JETIR)*, vol. 10, no. 6, pp. b658–b670, 2023.
- [44] A. S. Khan, A. Ali, G. Hussain, and M. Ilyas, “An experimental study on interfacial fracture toughness of 3-D printed ABS/CF-PLA composite under mode I, II, and mixed-mode loading,” *Journal of Thermoplastic Composite Materials*, vol. 34, no. 12, pp. 1599–1622, 2021, doi: 10.1177/0892705719874860.
- [45] A. Kholil et al., “Compression strength characteristics of ABS and PLA materials affected by layer thickness on FDM,” *Journal of Physics: Conference Series*, vol. 2377, Art. no. 012008, 2022, doi: 10.1088/1742-6596/2377/1/012008.
- [46] B. J. Lopes and J. R. M. d’Almeida, “Initial development and characterization of carbon fiber reinforced ABS for future additive manufacturing applications,” *Materials Today: Proceedings*, vol. 8, pp. 719–730, 2019.
- [47] A. Dhandapani et al., “Investigation of wear behavior in self-lubricating ABS polymer composites reinforced with glass fiber/ABS and glass fiber/carbon fiber/ABS hybrid,” *Lubricants*, vol. 11, Art. no. 131, 2023, doi: 10.3390/lubricants11030131.
- [48] M. Ranaiefar, M. Singh, and M. C. Halbig, “Additively manufactured carbon-reinforced ABS honeycomb composite structures and property prediction by machine learning,” *Molecules*, vol. 29, Art. no. 2736, 2024, doi: 10.3390/molecules29122736.
- [49] V. Mourya, S. P. Bhole, and P. G. Wandale, “Multiobjective optimization of tribological characteristics of 3D printed texture surfaces for ABS and PLA polymers,” *Journal of Thermoplastic Composite Materials*, vol. 37, no. 2, pp. 772–799, 2024, doi: 10.1177/08927057231185710.
- [50] V. Karupaiah et al., “Performance evaluation of 3D-printed ABS and carbon fiber-reinforced ABS polymeric spur gears,” *BioResources*, pp. 2796–2810, 2024, doi: 10.15376/biore.19.2.2796-2810.
- [51] N. Yu et al., “Effects of auxiliary heat on warpage and mechanical properties in carbon fiber/ABS composite manufactured by fused deposition modeling,” *Materials & Design*, Art. no. 108978, 2020, doi: 10.1016/j.matdes.2020.108978.
- [52] K. Ogi, T. Nishikawa, Y. Okano, and I. Taketa, “Mechanical properties of ABS resin reinforced with recycled CFRP,” *Advanced Composite Materials*, pp. 181–194, 2007, doi: 10.1163/156855107780918982.
- [53] V. Kovan, T. Tezel, H. E. Camurlu, and E. S. Topal, “Effect of printing parameters on mechanical properties of 3D printed PLA/carbon fibre composites,” *Materials Science. Non-Equilibrium Phase Transformations*, pp. 126–128, 2018.
- [54] K. Wang et al., “Flexure behaviors of ABS-based composites containing carbon and Kevlar fibers by material extrusion 3D printing,” *Polymers*, Art. no. 1878, 2019, doi: 10.3390/polym11111878.
- [55] V. S. Vakharia et al., “Effect of reinforcements and 3-D printing parameters on the microstructure and mechanical properties of acrylonitrile butadiene styrene (ABS) polymer composites,” *Polymers*, vol. 14, Art. no. 2105, 2022, doi: 10.3390/polym14102105.
- [56] A. Yankin et al., “Optimization of printing parameters to enhance tensile properties of ABS and nylon produced by fused filament fabrication,” *Polymers*, vol. 15, Art. no. 3043, 2023, doi: 10.3390/polym15143043.
- [57] P. Verma et al., “Essential work of fracture assessment of acrylonitrile butadiene styrene (ABS) processed via fused filament fabrication additive manufacturing,” *The International Journal of Advanced Manufacturing Technology*, vol. 113, pp. 771–784, 2021, doi: 10.1007/s00170-020-06580-4.
- [58] M. R. Khosravani et al., “Characterization of 3D-printed PLA parts with different raster orientations and printing speeds,” *Scientific Reports*, vol. 12, Art. no. 1016, 2022, doi: 10.1038/s41598-022-05005-4.
- [59] V. Cojocaru et al., “The influence of the process parameters on the mechanical properties of PLA specimens produced by fused filament fabrication—A review,” *Polymers*, vol. 14, Art. no. 886, 2022, doi: 10.3390/polym14050886.
- [60] M. T. Mansour, K. Tsongas, and D. Tzetzis, “The mechanical performance of 3D printed hierarchical honeycombs using carbon fiber and carbon nanotube reinforced acrylonitrile butadiene styrene filaments,” *MATEC Web of Conferences*, vol. 318, Art. no. 01049, 2020, doi: 10.1051/mateconf/202031801049.
- [61] H. Zhao et al., “An overview of research on fused deposition modeling three-dimensional printing process of continuous fiber reinforced composites,” *IOP Conference Series: Journal of Physics: Conference Series*, vol. 1213, Art. no. 052037, pp. 1–10, 2019, doi: 10.1088/1742-6596/1213/5/052037.
- [62] H. Kim, E. Park, S. Kim, B. Park, N. Kim, and S. Lee, “Experimental study on mechanical properties of single- and dual-material 3D printed products,” *Procedia Manufacturing*, vol. 10.
- [63] A. Parmiggiani, M. Prato, and M. Pizzorni, “Effect of the fiber orientation on the tensile and flexural behavior of continuous carbon fiber composites made via fused filament fabrication,” *The International Journal of Advanced Manufacturing Technology*, vol. 114, pp. 2085–2101, 2021, doi: 10.1007/s00170-021-06997-5.
- [64] M. Petousis et al., “Compressive response versus power consumption of acrylonitrile butadiene styrene in material extrusion additive manufacturing: The impact of seven critical control parameters,” *The International Journal of Advanced Manufacturing Technology*, vol. 126, pp. 1233–1245, 2023, doi: 10.1007/s00170-023-11202-w.
- [65] J. D. Kechagias and S. P. Zaoutsos, “An investigation of the effects of ironing parameters on the surface and compression properties of material extrusion components utilizing a hybrid-modeling experimental approach,” *Progress in Additive Manufacturing*, vol. 9, pp. 1683–1695, 2024, doi: 10.1007/s40964-023-00536-2.
- [66] Solidspace Technology LLP. 3D printing filament material technical properties. Nashik (MH): Solidspace Technology LLP.
- [67] 3DXTech. Technical data sheet: CarbonX™ carbon fiber ABS 3D printing filament. Rev 3.0.
- [68] Kristiawan RB, Imaduddin F, Ariawan D, Ubaidillah, Arifin Z. A review on the fused deposition modeling 3D printing: Filament processing, materials, and printing parameters. *Open Eng.* 2021 Jan;11(1):639–649. doi: 10.1515/eng-2021-0063.